JMIR Biomedical Engineering

Engineering for health technologies, medical devices, and innovative medical treatments and procedures
Volume 3 (2018), Issue 1 ISSN 2561-3278 Editor in Chief: Syed A. A. Rizvi, MD, PhD, MBA, MPH, BSN

Contents

Original Papers

Original Paper

Wireless Surface Electromyography and Skin Temperature Sensors for Biofeedback Treatment of Headache: Validation Study with Stationary Control Equipment

Anker Stubberud[1]; Petter Moe Omland[1,2], PhD; Erling Tronvik[1,3], PhD; Alexander Olsen[4,5], PhD; Trond Sand[1,3], PhD; Mattias Linde[1,3], PhD

[1]Department of Neuromedicine and Movement Science, Norwegian University of Science and Technology, Trondheim, Norway
[2]Department of Neurology and Clinical Neurophysiology, St Olavs Hospital, Trondheim, Norway
[3]National Advisory Unit on Headaches, Section of Neurology, St Olavs Hospital, Trondheim, Norway
[4]Department of Psychology, Norwegian University of Science and Technology, Trondheim, Norway
[5]Department of Physical Medicine and Rehabilitation, St Olavs Hospital, Trondheim, Norway

Corresponding Author:
Anker Stubberud
Department of Neuromedicine and Movement Science
Norwegian University of Science and Technology
Nevro Øst, Edvard Griegs Gate 8
Trondheim, 7030
Norway
Phone: 47 73 59 20 20
Email: ankers@stud.ntnu.no

Abstract

Background: The use of wearables and mobile phone apps in medicine is gaining attention. Biofeedback has the potential to exploit the recent advances in mobile health (mHealth) for the treatment of headaches.

Objectives: The aim of this study was to assess the validity of selected wireless wearable health monitoring sensors (WHMS) for measuring surface electromyography (SEMG) and peripheral skin temperature in combination with a mobile phone app. This proof of concept will form the basis for developing innovative mHealth delivery of biofeedback treatment among young persons with primary headache.

Methods: Sensors fulfilling the following predefined criteria were identified: wireless, small size, low weight, low cost, and simple to use. These sensors were connected to an app and used by 20 healthy volunteers. Validity was assessed through the agreement with simultaneous control measurements made with stationary neurophysiological equipment. The main variables were (1) trapezius muscle tension during different degrees of voluntary contraction and (2) voluntary increase in finger temperature. Data were statistically analyzed using Bland-Altman plots, intraclass correlation coefficient (ICC), and concordance correlation coefficient (CCC).

Results: The app was programmed to receive data from the wireless sensors, process them, and feed them back to the user through a simple interface. Excellent agreement was found for the temperature sensor regarding increase in temperature (CCC .90; 95% CI 0.83-0.97). Excellent to fair agreement was found for the SEMG sensor. The ICC for the average of 3 repetitions during 4 different target levels ranged from .58 to .81. The wireless sensor showed consistency in muscle tension change during moderate muscle activity. Electrocardiography artifacts were avoided through right-sided use of the SEMG sensors. Participants evaluated the setup as usable and tolerable.

Conclusions: This study confirmed the validity of wireless WHMS connected to a mobile phone for monitoring neurophysiological parameters of relevance for biofeedback therapy.

(JMIR Biomed Eng 2018;3(1):e1) doi:10.2196/biomedeng.9062

KEYWORDS

biofeedback; mobile phone; app; migraine; pediatric

Introduction

In the emerging era of mobile health (mHealth) and technology, the use of wearable sensors and mobile phone health apps has recently gained attention. This has led to a subcategory of health informatics, labeled mHealth, encompassing the use of mobile phones for medical purposes [1]. In addition to these apps, there is also a wide array of wearable health monitoring sensors (WHMS) [2],which represent a means for patients to access real-time data from a broad range of physiological parameters at home [3-5], thus enabling extensive data acquisition [6]. mHealth is of special interest to the younger generation, which is constantly exposed to and familiarized with such technology. It is also increasing in popularity within the field of headache care and research. In particular, mobile phone–based headache diaries are frequently used [7]. However, there is a potential for extending this mobile technology into the preventive treatment of headache disorders, such as migraine. The bulk of current mHealth research focuses on chronic conditions and delivery of self-educational treatment [8], fitting the description of behavioral headache treatments. Biofeedback, one of the several behavioral headache treatments, is well established and empirically supported [9]. Systematic reviews with meta-analyses demonstrated that biofeedback is effective as a migraine prophylaxis in both the adult and pediatric populations [10,11]. However, the treatment is both time-consuming and costly and therefore not readily available for those in need. Thus, a more optimal approach for behavioral headache treatment has long been sought [12,13]. Biofeedback has the potential to exploit the recent advances in mHealth technology [14,15]. All the while, biofeedback mHealth solutions for other purposes, such as exercise and postcancer swallowing exercises, are being developed [16,17].

Modalities proven effective in biofeedback treatment for headache disorders include surface electromyography (SEMG) and peripheral skin temperature. Both modalities are common in the current development of WHMS [2] and may serve as natural elements in the implementation of biofeedback solutions. Nevertheless, such WHMS sensors have not been validated for use in neurophysiological monitoring for the purpose of biofeedback therapy.

The aim of this study was to assess the validity of WHMS for measuring SEMG and peripheral skin temperature in combination with a mobile phone app. This proof of concept would form the basis for the development of a novel, innovative mHealth system for biofeedback therapy for young persons with primary headache.

Methods

Study Design

In the first phase of the study, we identified suitable WHMS and developed the preliminary software. In the second phase of the study, we recruited healthy volunteers to establish the validity of the chosen WHMS. The study was exploratory in nature, with the main aim to evaluate the validity of the chosen WHMS by assessing the agreement compared with stationary neurophysiological equipment following recommended guidelines for agreement studies [18].

Identification of Sensors

The inclusion criteria and requirements for suitable sensors were (1) wireless setup, (2) small size, (3) low weight, (4) simple to use compared with standard clinical equipment, and (5) low cost.

Software Development

The first version of the app was created as a minimal viable product (MVP). This preliminary version was programmed to serve as the starting point of iterative and incremental rounds of testing [19], allowing subsequent development and fine-tuning of the user interface and software components in an upcoming usability study.

Participants

We considered a sample size of 18 to be sufficient, based on the model for sample size determination in reliability studies presented by Bonett [20] (Multimedia Appendix 1). We set out to recruit 20 healthy volunteers to account for potential dropouts. Participants were recruited as a convenience sample by actively seeking out young individuals from the local research and student community. Exclusion criteria were reduced hearing, vision, or sensibility, and severe neurologic or psychiatric disease.

Equipment

TheNeckSensor (EXPAIN, Oslo, Norway) was selected as the wireless WHMS to measure muscle tension. This is a small, compact bipolar SEMG sensor, with a single SR-R adhesive gel patch containing both electrodes (total patch area, 19.8 cm^2), and no patient ground electrode. For wireless measurement of temperature, we selected the PASPORT Skin/Surface Temperature Probe, PS-2131, combined with PASPORT Temperature sensor, PS-2125, and AirLink, PS-3200 (Pasco, Roseville, CA, USA). Both the sensors transmitted signals via Bluetooth Smart/4.0.

As the stationary equipment, the following AD Instruments (Dunedin, New Zealand) setup was used: (1) SMEG signals recorded with 5-Lead Shielded Lead Wires (MLA2505) and 5-Lead Shielded BioAmp cable (MLA2540) attached to Red Dot 2560 electrodes with a silver/silver-chloride 3.48 cm^2 sensor area (3M Health Care, Germany) fed through a Dual BioAmp, FE135, and PowerLab 8/35; (2) equivalent lead wires, cables, and electrodes for registration of an electrocardiogram (ECG) through a separate Dual BioAmp; and (3) temperature registered through Skin Temperature Pod and Probe, ML309 + MLT422/A fed through PowerLab. The recordings were visualized and analyzed using the LabChart 8 software (AD Instruments, Dunedin New Zealand) installed on a Dell Latitude E4310 laptop.

Experimental Procedure

Participants were seated in a recliner at a 90 degree angle in the neurophysiological laboratory. The 2 electrodes from the NeckSensor were placed over the upper fibers of the right trapezius muscle midway along the line between the spinous

process C7 and the acromion [21,22]. Since simultaneous registrations of SEMG signals from the same location with different sets of surface electrodes are not possible, one set of electrodes from the stationary equipment was placed 2 cm cranially of the NeckSensor, and the other set was placed 2 cm caudally. The interelectrode distance was 4 cm. The "patient ground" electrode for the stationary equipment was placed over the spinous process C7 (Figure 1). The skin beneath the stationary electrodes was washed with alcohol swabs. The 2 skin temperature sensors were attached, without touching each other, to the volar pad of the distal phalange on the second finger with sticky tape, with the stationary sensor placed radially of the 2 sensor electrodes.

Figure 1 shows the scheme of the electrode placements over the upper trapezius fibers. The wireless sensor electrode pair was placed first, midway in the line between the acromion and the spinous process C7. One of the two pairs of stationary sensor electrodes was placed cranially, whereas the other was placed caudally of the wireless sensor electrode pair. The interelectrode distance for each pair was 4 cm.

Initially, each participant was asked to relax for 5 min to allow the skin temperature to increase during relaxation. Relaxation was achieved by asking the participant to do nothing and sit still on the recliner. This served to give a baseline (relaxed) muscle tension measurement. Relaxed trapezius muscle tension (baseline) was recorded in the last 30 s of relaxation. Thereafter, the temperature sensors were detached to allow the measurement of room temperature for the remainder of the procedure. Subsequently, the participant was instructed to complete a series of exercises to activate the upper fibers of the trapezius muscle. Arbitrary angle isometric maximal voluntary contraction (MVC), through shoulder elevation, was completed in 3 repetitions, each lasting for 6 s [22-25]. The SEMG and force were simultaneously registered. The force was recorded by a dynamometer (Manual Muscle Tester, Lafayette Instruments, USA) attached to a fixed sling placed over the acromion. Subsequently, the participant was asked to complete similar sets of contractions at 50% (VC50) and 25% (VC25) of maximal contraction guided by a sound signal from the dynamometer elicited at a corresponding set force. Finally, the participant was asked to complete 4 repetitions of static contractions (15 s each) performed by abducting both shoulders to a 90 degree angle and holding them against gravity [22].

After completing the exercises, the participant was asked to answer a 5 - item user evaluation questionnaire. Of these, 3 questions had reply options on a 5 - point Likert scale, ranging from "Very dissatisfied" to "Very satisfied," while the remaining 2 questions were open for free comments (Table 1).

Figure 1. Electrode placement.

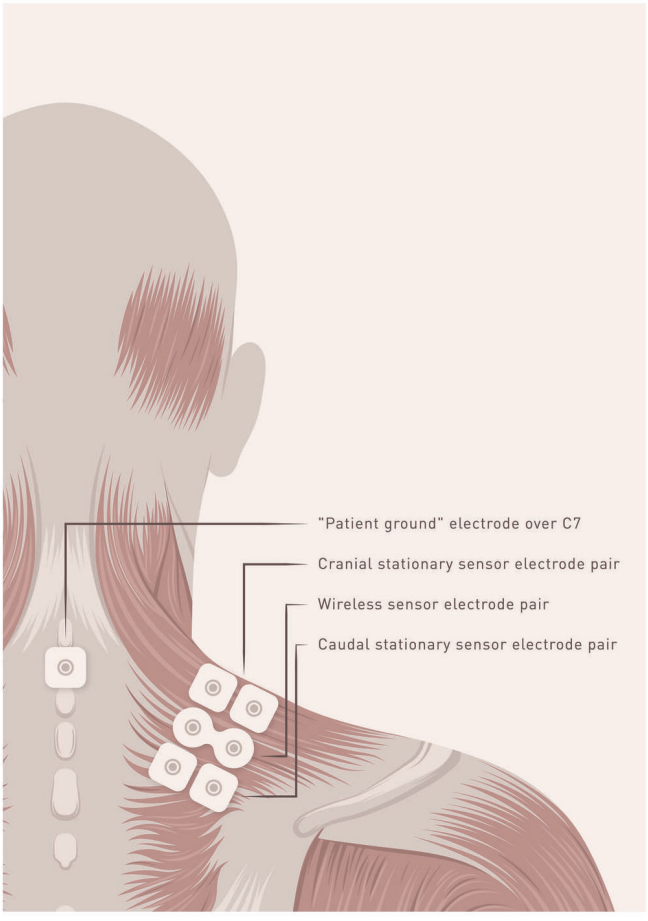

Table 1. Evaluation questionnaire.

Item	Question
1	Did you perceive the wireless sensors as practical to use?
2	To what degree did you feel that the use of shoulder-musculature reflected the feedback in the app?
3	Do you recognize the wireless sensors as safe to use?
4	Did you experience any undesirable harmful effects (if yes, please explain)?
5	Do you have any further comments (if yes, please explain)?

Data Management

The NeckSensor uses a 12 - bit ADC resolution sampled at 1024 Hz with a third order 10 - 480 Hz active bandpass filter. The sensor was programmed to calculate and transmit mean square values internally, with a window width of 40 ms, with no overlap, and a frequency of 25 Hz in order not to overload the Bluetooth capacity. The PowerLab sampled the SEMG signals at 2000 Hz with a fourth order Bessel lowpass filter at 500 Hz and a first order high pass filter at 10 Hz. In addition, a 50 Hz notch analog filter was applied [26]. All stationary recordings were evaluated visually for the presence of ECG artifacts. If found, these were to be corrected by removing the spike-correlated area in the SEMG signal and subsequently replacing the gap with surrounding SEMG activity.

First, the stationary readings were root mean square (RMS) rectified and then averaged over the two sets of electrodes to avoid phase-cancellations. The RMS value was calculated from the mean square values of the wireless sensors. The RMS values for each muscle contraction exercise to be used in the analyses were calculated as the mean of the repetitions for both equipment sets. For the temperature measurements, we calculated the difference in temperature from the start to the end of relaxation and the difference between the temperature at the end of relaxation and room temperature.

Statistics

The means and SD for the RMS values during trapezius muscle exercises and the chosen data temperature points were calculated. Systematic differences between stationary and wireless equipment were assessed with the Wilcoxon signed-rank test.

Mean difference (MD) and limits of agreement (LOA), together with Bland-Altman plots were used as descriptive tools [27].We calculated the intraclass correlation coefficient (ICC) with a two-way, mixed-effects consistency of agreement model. Coefficients for both individual and average agreement were presented. In addition, we calculated the Lin concordance correlation coefficient (CCC) [28-30]. For the ICC and CCC analyses, the data was first transformed to meet assumptions for a two-way analysis of variance model. Then the data was transformed by calculating the natural logarithm after adding 0.1 as a constant to adjust for values being close to zero. The ICC values were interpreted as suggested by Cicchetti et al [31], that is, unacceptable or poor (.00 - .40), fair (.41 - .60), good (.61 - .75), and excellent (.75 - 1.00). All data were analyzed by using the statistical package Stata version 14 (StataCorp, College Station, TX, USA).

Results

Sensors and Software

The WHMS fulfilling the predefined requirements were identified through pragmatic Internet-searches. The MVP version of the app used in the experimental procedure was programmed to receive data from the wireless sensors and feed raw data back to the user. The raw data were presented as two columns increasing in height with increase in muscle tension and temperature, respectively. The app was programmed to allow connection of any WHMS using Bluetooth.

Participants

A total of 20 healthy participants were recruited and completed the experimental procedure. Of these, 12 were male participants, and their mean age was 24.7 years (SD 2.7, range 18 - 29 years).

Surface Electromyography Sensor Agreement

We observed no ECG artifacts in the SEMG recordings (Figure 2). Hence, the ECG-related elements were not removed from the SEMG recordings.

Figure 2 shows the raw data of the SEMG activity for the wireless sensor (red), anterior stationary sensor (blue), and posterior stationary sensor (green) from a 24-year-old male participant. The marked areas indicate where the different exercises are performed. The figure exemplifies the absence of ECG artifacts and the similarity of the signals.

Means and standard deviations of the RMS values for the trapezius muscle exercises are presented in Table 2. The wireless sensor showed a lower voltage during trapezius muscle exercises than during all contraction periods and at baseline.

Table 3 summarizes the MD in millivolts (mV) between stationary and wireless equipment with corresponding LOA, for each of the exercises. Compared with the wireless equipment, the stationary equipment indicated a systematically higher voltage during MVC (0.25 mV), VC50 (0.11 mV), VC25 (0.06 mV), static hold (0.07 mV), and baseline (0.04 mV). A Bland-Altman plot, visually presenting the MD and LOA for VC25, is shown in Figure 3. Table 3 also summarizes the ICC and CCC values for the SEMG equipment comparisons.

Figure 2. Raw surface electromyography (SEMG) data. ECG: electrocardiogram; MVC: maximal voluntary contraction; RMS: root mean square; VC50: voluntary contraction at 50% force; VC25: voluntary contraction at 25% force.

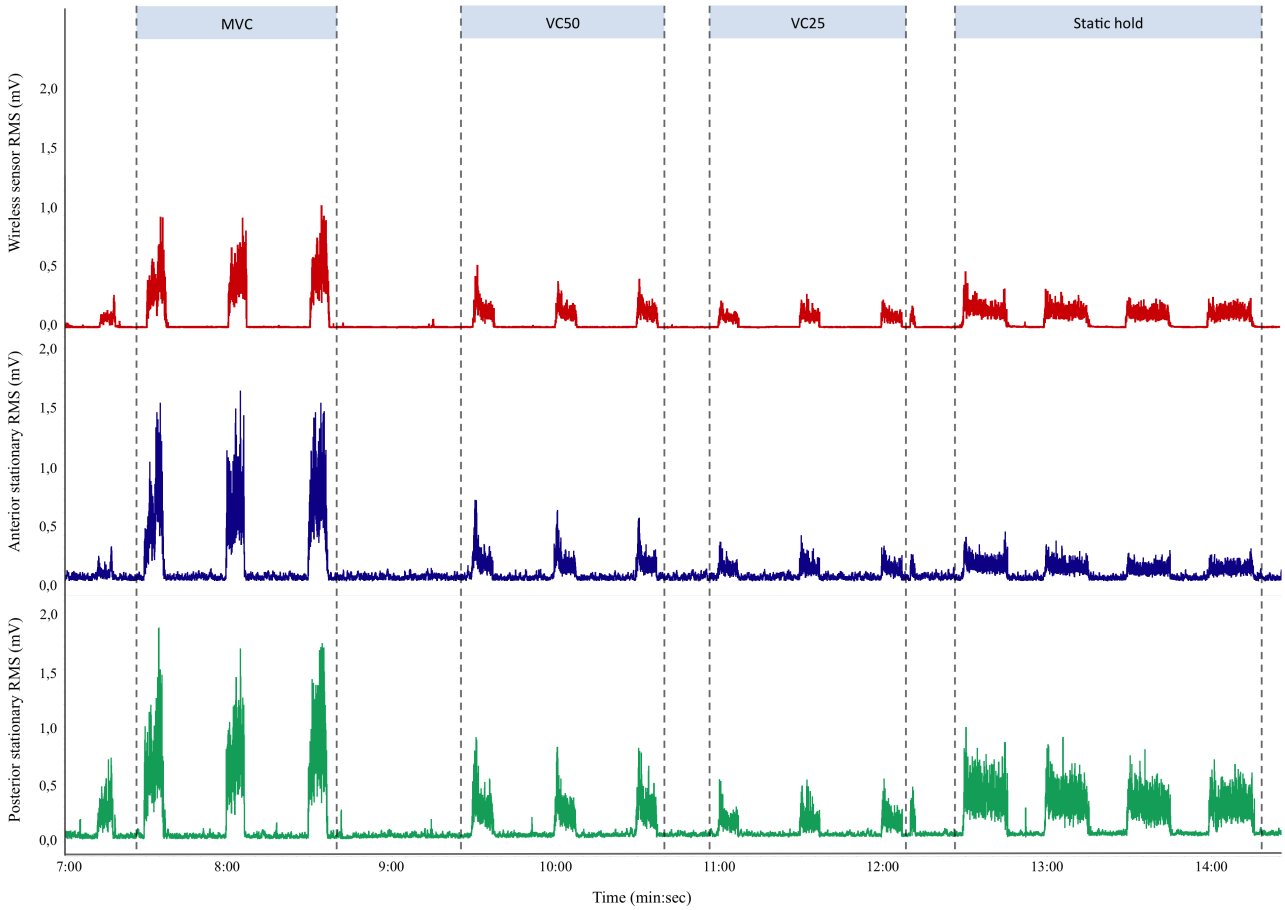

Table 2. Comparison of the means for stationary and wireless equipment.

Exercise	Stationary equipment (SD)	Wireless equipment (SD)	Z-value (*P* value)[a]
MVC[b]	0.62[c] (0.25)	0.37 (0.15)	3.73 (<.001)
VC50[d]	0.26 (0.11)	0.15 (0.06)	3.92 (<.001)
VC25[e]	0.15 (0.05)	0.09 (0.05)	3.73 (<.001)
Static hold	0.16 (0.06)	0.08 (0.03)	3.85 (<.001)
Baseline	0.045 (0.004)	0.01 (0.002)	3.92 (<.001)
Start temperature	28.8[f] (3.4)	28.8 (3.3)	0.75 (=.46)
End temperature	30.7 (3.6)	31.5 (4.0)	3.4 (<.001)
Room temperature	23.0 (0.3)	23.6 (0.4)	3.9 (<.001)

[a]Z-value from Wilcoxon signed-rank test.
[b]MVC: maximal voluntary contraction.
[c]Mean voltage in millivolts RMS.
[d]VC50: voluntary contraction at 50% force.
[e]VC25: voluntary contraction at 25% force.
[f]Mean temperature in degrees Celsius.

Table 3. Indices of agreement between stationary and wireless equipment.

Exercise	Mean difference	Limits of agreement	ICC[a] (95% CI) individual	ICC (95% CI) average	CCC[b] (95% CI)
MVC[c]	0.25[f]	−0.12 to 0.61	.81 (0.57 - 0.92)	.89 (0.73 - 0.96)	.52 (0.30 - 0.73)
VC50[d]	0.11	−0.04 to 0.27	.81 (0.57 - 0.92)	.89 (0.73 - 0.96)	.44 (0.23 - 0.64)
VC25[e]	0.06	−0.03 to 0.15	.66 (0.31 - 0.85)	.79 (0.47 - 0.92)	.37 (0.14 - 0.60)
Static hold	0.07	−0.02 to 0.16	.58 (0.19 - 0.81)	.73 (0.32 - 0.89)	.26 (0.06 - 0.45)
Baseline	0.04	0.03-0.04	.50 (0.09 - 0.77)	.67 (0.16 - 0.87)	.01 (0.00 - 0.01)
Start to end temperature	−0.77[g]	−1.90 to 0.35	.96 (0.91 - 0.99)	.98 (0.95 - 0.99)	.90 (0.83 - 0.97)
End to room temperature	−0.23	−1.74 to 1.28	.98 (0.95 - 0.99)	.99 (0.97 - 1.0)	.98 (0.96 - 1.0)

[a]ICC: intraclass correlation coefficient.

[b]CCC: concordance correlation coefficient.

[c]MVC: maximal voluntary contraction.

[d]VC50: voluntary contraction at 50% force.

[e]VC25: voluntary contraction at 25% force.

[f]Mean voltage in millivolts RMS.

[g]Mean temperature in degrees Celsius.

Figure 3. Surface electromyography (SEMG) sensor agreement. mV: millivolts; RMS: root mean square.

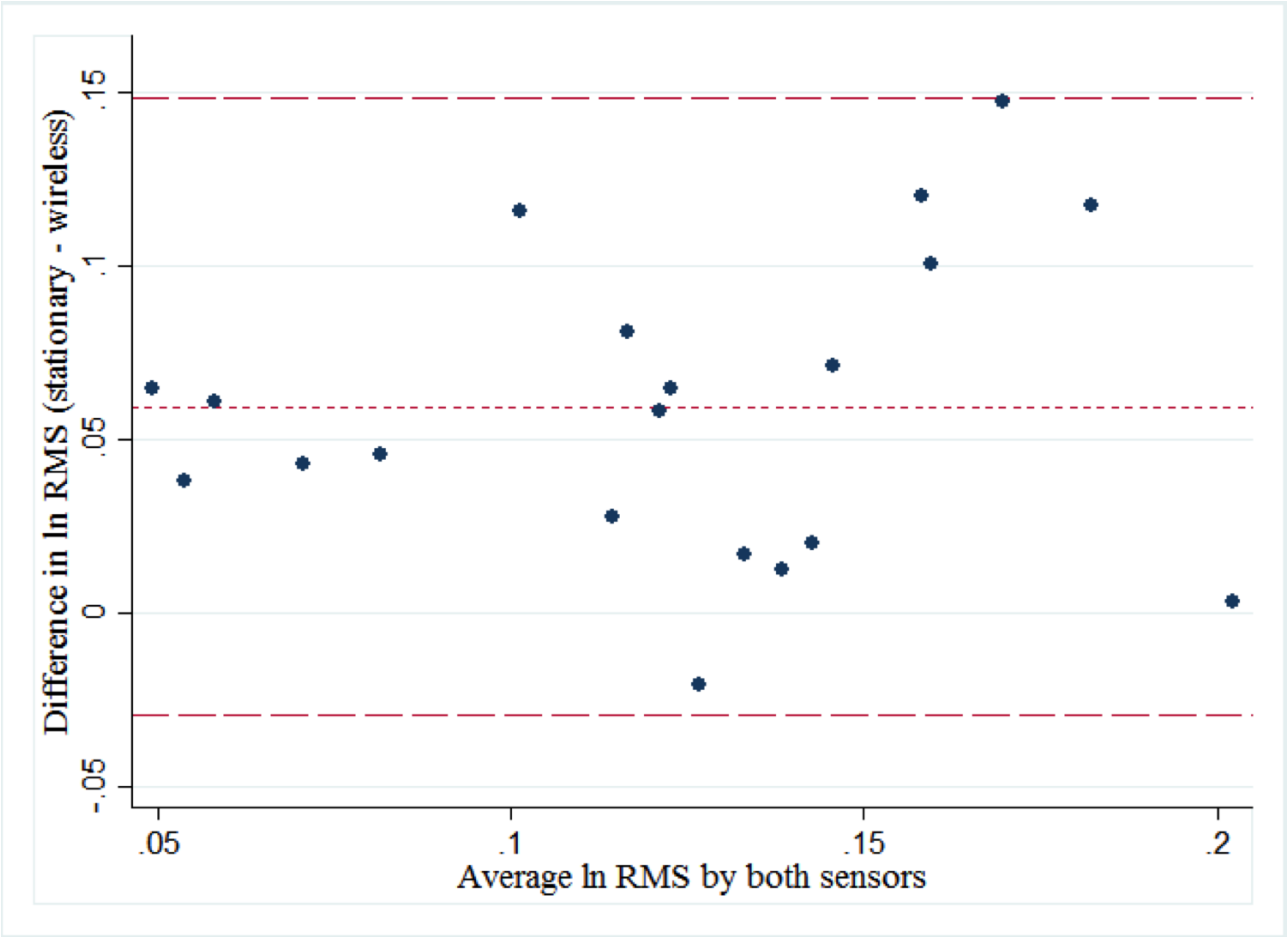

Excellent agreement was found for MVC (ICC .81, 95% CI 0.57 - 0.92) and VC50 (ICC .81, 95% CI 0.57 - 0.92). Good agreement was found for VC25 (ICC .66, 95% CI 0.31 - 0.85). Fair agreement was found for static hold (ICC .58, 95% CI 0.19 - 0.81) and baseline (ICC .50, 95% CI 0.09 - 0.77). All participants displayed a decrease in voltage from MVC to VC50, from VC50 to VC25, and from static hold to baseline for both sets of equipment, with the exception of one participant who had a small increase (0.03 mV) in voltage from VC50 to VC25 registered on the stationary equipment (Figure 4).

Figure 3 shows Bland-Altman plot assessing the agreement between stationary and wireless SEMG sensors during voluntary contraction at 25% force. The x-axis represents the average of the two parallel measurements. The y-axis represents the corresponding difference between the 2 measurements. The values are indicated in millivolt RMS.

Figure 4 is a line graph showing the SEMG readings for each participant during MVC, VC50, VC25, static hold, and baseline. The top panel indicates readings with the stationary equipment. The bottom panel indicates readings with the wireless equipment. The values are indicated in millivolt RMS.

Peripheral Skin Temperature Sensor Agreement

Means and standard deviations of the temperature measurements at the 3 selected time points are shown in Table 2. The start temperature between the 2 sets of equipment did not differ significantly (P=.46), but the wireless sensor indicated a higher temperature at the end of relaxation (P<.001) and at room temperature (P<.001; Table 2).

The between-equipment MDs for changes in the temperature are presented in Table 3, along with the LOA and agreement indices. A Bland-Altman plot visually representing the MD and LOA for temperature change during relaxation is depicted in Figure 5. Excellent agreement was found for the change in temperature during relaxation (CCC .90, 95% CI 0.83 - 0.97) and from end of relaxation to room temperature (CCC .98, 95% CI 0.96 - 1.0). A rise in temperature was detected among 17 participants on the stationary equipment, and among 18 participants on the wireless equipment. Moreover, a rise in temperature of more than 1°C was detected among 15 participants on both equipment sets (Figure 6).

Figure 5 is a Bland-Altman plot showing the agreement between stationary and wireless equipment for the change in temperature from start to end of relaxation. The x-axis represents the average of the 2 parallel measurements. The y-axis represents the corresponding difference in measurements. The values are in degrees Celsius.

Figure 6 is a line graph showing temperature readings for each participant at the start and end of relaxation and at room temperature. The upper panel represents readings with the stationary equipment. The lower panel represents readings with the wireless equipment. The values are in degrees Celsius.

Evaluation Questionnaire

In total, 19 of the 20 participants perceived the use of wireless sensors as practical (n=14) or very practical (n=5). Likewise, the absolute majority of participants reported that the app feedback reflected the use of shoulder musculature to a large (n=9) or a very large (n=9) degree. All participants regarded the use of wireless sensors as safe (n=2) or very safe (n=18). In contrast, 2 of the 20 participants reported undesirable, harmful effects, with both stating that the removal of the electrodes attached to the stationary equipment was unpleasant.

Figure 4. Surface electromyography (SEMG) sensor line graphs. mV: millivolts; MVC: maximal voluntary contraction; RMS: root mean square; VC50: voluntary contraction at 50% force; VC25: voluntary contraction at 25% force.

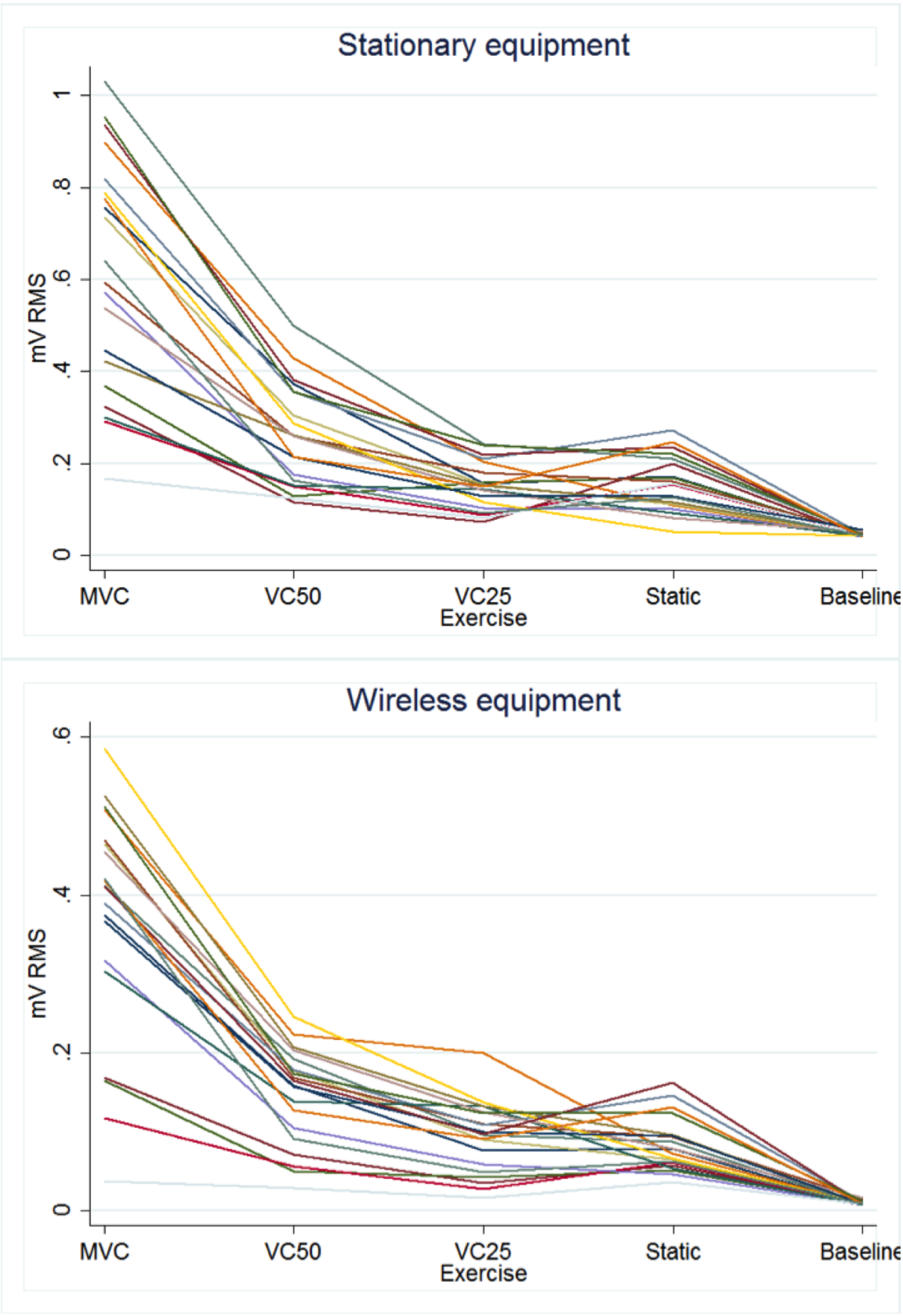

Figure 5. Temperature sensor agreement. mV: millivolts; RMS: root mean square.

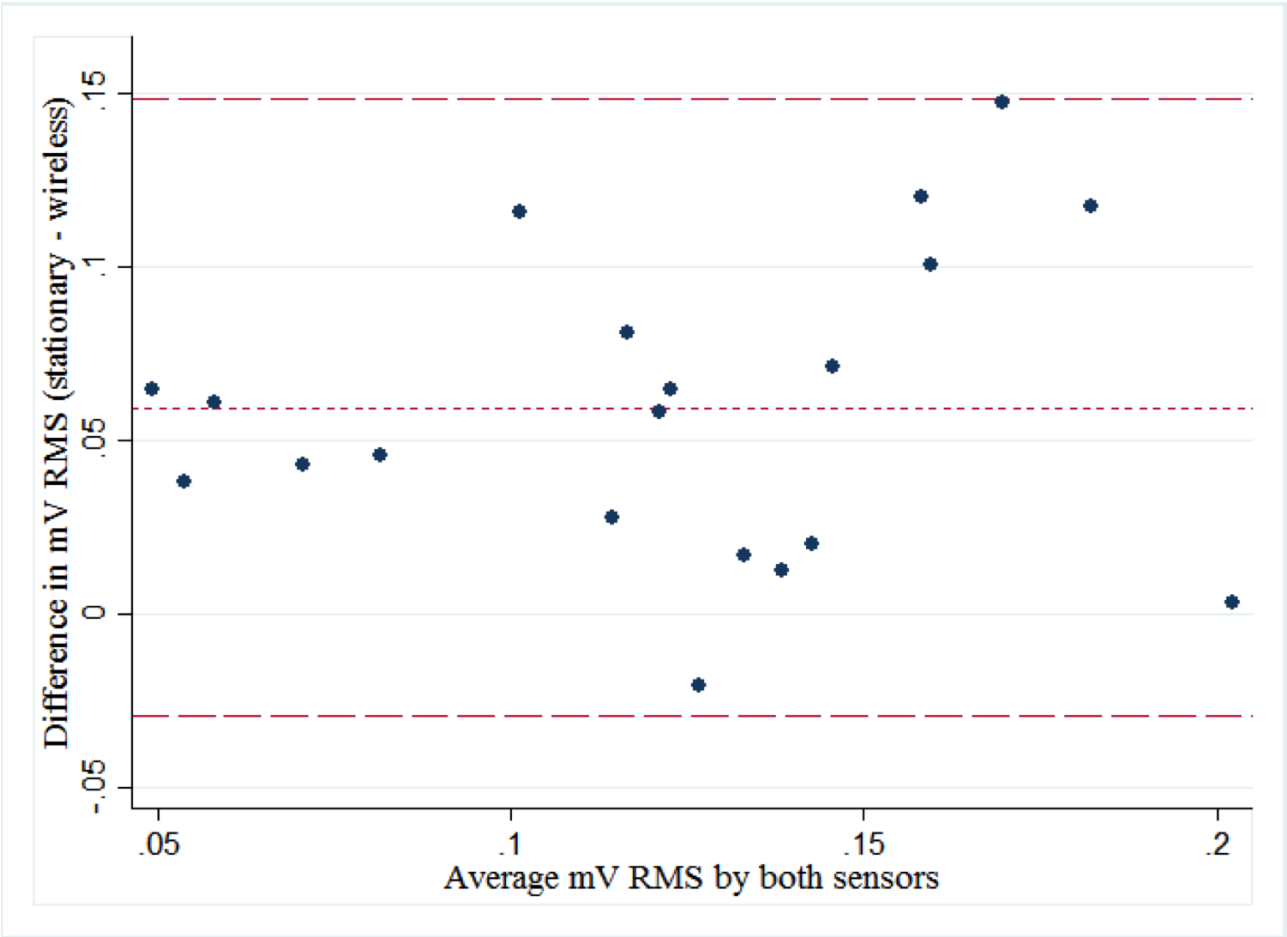

Figure 6. Temperature sensor line graphs.

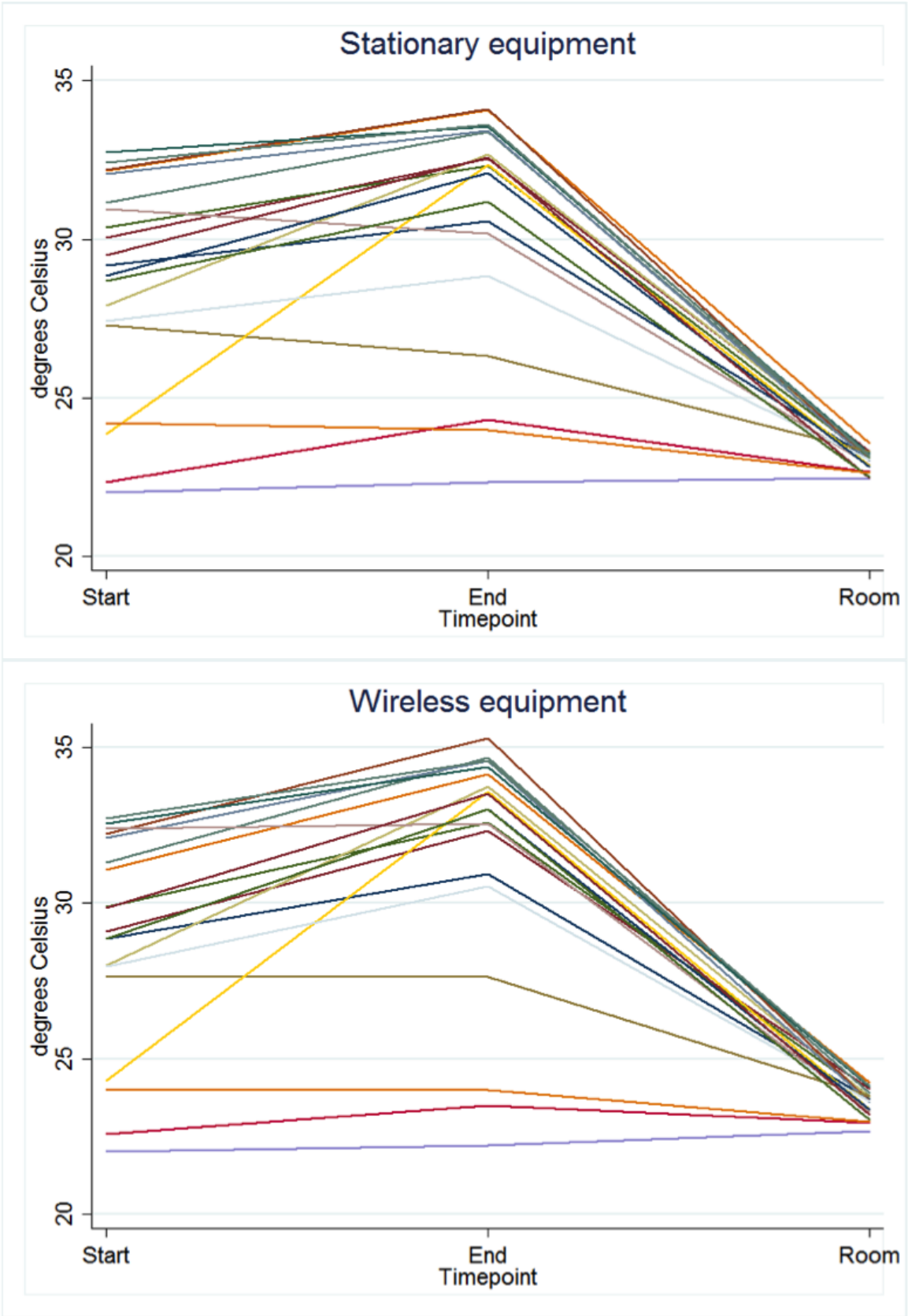

Discussion

Principal Findings

This study aimed to provide a proof of concept for using a mobile phone and WHMS for biofeedback purposes, in a fashion similar to phase I-II development of new drug treatments [32]. We chose to investigate temperature and SMEG because they are the most commonly used biofeedback modalities [11] and are shown to be especially effective in adolescents [33]. We identified sensors fulfilling a set of predefined criteria that were considered necessary for the sensors to gain acceptance among patients, and thus these sensors were used [34]. The choice of sensors was arbitrary, as long as the predefined criteria were met. Even though the use of other temperature and SEMG sensors would not yield identical results, we argue that our approach has provided a proof of concept.

We found that the use of a wireless temperature sensor had almost perfect agreement regarding the change in finger temperature during relaxation. Furthermore, the use of a wireless SEMG sensor had a fair to excellent agreement for measuring tension in the trapezius muscle. We noted that the wireless SEMG consistently showed a lower voltage than the stationary equipment. The SEMG sensors showed excellent agreement during MVC and VC50, good agreement during VC25, and fair agreement during static hold and baseline. However, under the assumption that the stationary equipment was the most sensitive, it is not surprising that the calculated agreement decreased slightly at lower activity levels since random and equipment-generated noise constituted a larger part of the signal at low EMG-levels. Nonetheless, the wireless SEMG sensor registered consistent changes in muscle tension. We observed no ECG artifacts in the SEMG recordings. Therefore, it can be assumed that the ECG artifacts do not have a relevant influence on the SEMG recorded from closely placed bipolar electrodes on the right shoulder. Moreover, the safety and usability of the setup were highly satisfactory. In conclusion, the wireless sensors are well suited for biofeedback purposes.

Strengths and Limitations

The proper sample size for the study was assessed before recruiting participants (Multimedia Appendix 1). Traditionally, a sample of 15 to 20 participants is deemed sufficient for reliability studies [35]. However, the use of more precise calculations of sample sizes has been previously suggested [36]. Therefore, we used a CI estimation model suggested by Bonett [20] to determine the minimum sample size required. Due to the interindividual variation in our findings, the analyses would possibly have benefited from having a larger sample size because we did not obtain a predefined CI for all analyses.

There is a large degree of variability in individual human anatomical properties that may influence SEMG readings. This includes the thickness of fatty tissues, resting muscle length, velocity of contraction, muscle cross-sectional area, fiber type, posture change, interelectrode distance, skin impedance, age, and sex [22]. We chose to combine the recordings for the 2 pairs of stationary sensor electrodes to approximate the muscle activity of the wireless sensor placed in between. The relative spread of the electrode pairs may have led to EMG crosstalk, and muscle contraction exercises performed by untrained participants may have additionally resulted in movement artifacts, and suboptimal and varying performances [37]. The abovementioned factors may all have limited the precision of our measurements and contributed to a larger degree of interindividual differences, thus lowering individual ICC and CCC values for SEMG agreement. Likewise, the placement of the 2 temperature sensors beside each other on the finger might have led to differences in measurements. Figure 5 shows 1 outlier that displayed a larger increase in temperature by 1°C with the stationary equipment than with the wireless equipment. This differs from the majority that displayed the largest temperature increase with the wireless equipment. Nevertheless, LOA of ±1.5°C is still acceptable [38].

The SEMG signals usually have a frequency distribution with significant energy up to 400 to 500 Hz, requiring a sampling frequency of at least 1000 Hz (preferably 2000 Hz) to meet the Nyquist rate (2 times higher signal frequency) and avoid the so-called aliasing [39]. However, it is known that oversampling above this critical Nyquist rate does not significantly improve the signal quality [40] but will likely lead to higher cost and size of the sensor. The SEMG signals are usually bandpass filtered at 10 to 500 Hz [41], which we consequently chose to do for both setups. Furthermore, we observed that the notch filter, at 50 Hz, for the stationary equipment seemed to be saturated during recordings. After analog filtering, sine waves of 20 ms duration were still present. This may be explained by power-line noise, despite the use of a notch filter [42]. The wireless sensor also applies a notch filter at 50 Hz, which increases the signal-to-noise ratio. In total, we concluded that the wireless SEMG sensor applies appropriate signal processing settings.

We chose different statistical methods for assessing agreement to evaluate different properties of the wireless sensors. The Wilcoxon signed-ranks tests, together with the Bland-Altman plot and LOA, assess the degree of systematic differences and expected variance between measurements. A two-way, mixed-effect ICC model [43] ignores the element of rater variance (raters fixed as the 2 equipment sets), and the estimate can thus serve as an index of consistency [28,30,44,45]. This is useful to assess agreement when having mean differences between 2 measurement methods. We reported both individual and average ICC values, as the average value becomes useful when a large degree of interindividual variance exists or if individual readings are considered unreliable [30]. On the other hand, we also calculated the CCC to evaluate the degree of absolute agreement, that is, the 2 measurement methods showing identical values.

Interpretation

We have compared the WHMS with a gold standard; however, this does not imply that the gold standard is without measurement error. Thus, some lack of agreement is inevitable [46]. As pointed out by Bland and Altman [47], one should keep in mind that correlation coefficients alone do not assess interchangeability of measurement methods. The acceptable level of agreement in order to claim validity is a clinical decision. Considering the intended use of the chosen sensors,

a high degree of absolute agreement is not a necessity, but consistency of agreement is important. We certainly observed that there exists variance in the data, leading to a low degree of absolute agreement. On the other hand, SEMG readings changed similarly and as expected through the experimental procedure for each participant, despite dissimilarities between the 2 equipment sets. This consistency is indeed supported by excellent to fair agreement of ICC values. Furthermore, the wireless SEMG sensor was less reliable at lower voltage, at least in terms of absolute agreement, when compared with our gold standard. A well-designed SEMG setup usually produces a system noise of about 1% of the MVC [48]. Our stationary equipment baseline showed 7% of MVC, which means that there was some inherent noise in the gold standard setup. In contrast, the baseline readings of the wireless sensors amounted to 3% of MVC, which in part may explain the increasing deviation at lower voltages.

Although the SEMG sensor did not demonstrate excellent agreement in all analyses, both SEMG and temperature WHMS appear to be suited for app-based biofeedback. Interestingly, 15 out of 20 participants (75%) managed to raise their temperature by more than 1°C during a single naive session indicating that the setup was simple to master. Moreover, all participants had similar changes in muscle tension through the sets of exercises. However, it is unlikely that the users will be able to decrease their muscle tension throughout the entire duration of a biofeedback session [49]. This means that detecting a change in tension is more important than the absolute values. In line with this, it was recently shown that the feedback itself is more important than lowering muscle tension in the treatment of headache [50]. Taken together, these findings imply that perfect sensor agreement in itself is not a prerequisite for an app-based biofeedback platform. The main focus of app-based biofeedback should be directed at the development of high-quality feedback mechanisms and user interfaces.

Prospects for Future Research

This study confirmed the usability of WHMS in a biofeedback setting and established partial evidence for an upcoming biofeedback app. At any rate, the scientific validation of the sensor is of utmost importance for the value and effectiveness of a future treatment program. The choice to use an MVP app to assess agreement enables iterative and incremental developments. Future research should be carried out to establish further the basis for the use of WHMS for medical purposes in the emerging era of health informatics and mHealth. As an example, similar validation of heart rate variability measurements, which is of interest in biofeedback treatment, has been conducted [51,52,53]. We are currently exploring the user interface and assessing the usability of the app among adolescents with migraine.

Conclusions

This study confirmed the validity of wireless WHMS connected to a mobile phone for monitoring neurophysiological parameters of relevance for biofeedback therapy.

Acknowledgments

The authors wish to thank all the volunteers for participating in the study. The study was funded by strategic seeding grants from the Faculty of Medicine, NTNU Norwegian University of Science and Technology. We would also like to thank Searis AS for the fruitful collaboration and for their help with programming the app, EXPAIN AS for supplying SEMG sensors for use in the study, and the personnel at the Department of Neurophysiology, St Olavs Hospital, for their support with the experimental procedures.

Conflicts of Interest

Anker Stubberud has participated as a nonpaid member of an Expert Panel advising EXPAIN AS during the final phases of product development. Should the research result in a commercially available product, the university and authors may benefit financially from future intellectual property rights.

Multimedia Appendix 1

Sample size determination.

[PDF File (Adobe PDF File), 32KB - biomedeng_v3i1e1_app1.pdf]

References

1. Kay M, Santos J, Takane M. Who.int. 2011. mHealth: new horizons for health through mobile technologies URL: http://www.who.int/goe/publications/goe_mhealth_web.pdf [accessed 2018-02-13] [WebCite Cache ID 6xCFk9ovq]
2. Pantelopoulos A, Bourbakis NG. A survey on wearable sensor-based systems for health monitoring and prognosis. IEEE Trans Syst Man Cybern C Appl Rev 2010;40(1):1-12. [doi: 10.1109/TSMCC.2009.2032660]
3. Dobkin BH, Dorsch A. The promise of mHealth: daily activity monitoring and outcome assessments by wearable sensors. Neurorehabil Neural Repair 2011;25(9):788-798 [FREE Full text] [doi: 10.1177/1545968311425908] [Medline: 21989632]
4. Hanson MA, Powell Jr HC, Barth AT, Ringenberg K, Calhoun BH, Aylor JH, et al. Body area sensor networks: challenges and opportunities. Computer 2009;42(1):58-65.

5. Schüll ND. Data for life: wearable technology and the design of self-care. BioSocieties 2016;11(3):317-333 [FREE Full text]
6. Lupton D. Quantifying the body: monitoring and measuring health in the age of mHealth technologies. Crit Public Health 2013;23(4):393-403. [doi: 10.1080/09581596.2013.794931]
7. Hundert AS, Huguet A, McGrath PJ, Stinson JN, Wheaton M. Commercially available mobile phone headache diary apps: a systematic review. JMIR Mhealth Uhealth 2014;2(3):e36 [FREE Full text] [doi: 10.2196/mhealth.3452] [Medline: 25138438]
8. Fiordelli M, Diviani N, Schulz PJ. Mapping mHealth research: a decade of evolution. J Med Internet Res 2013;15(5):e95 [FREE Full text] [doi: 10.2196/jmir.2430] [Medline: 23697600]
9. Penzien DB, Irby MB, Smitherman TA, Rains JC, Houle TT. Well-established and empirically supported behavioral treatments for migraine. Curr Pain Headache Rep 2015 Jul;19(7):34. [doi: 10.1007/s11916-015-0500-5] [Medline: 26065542]
10. Stubberud A, Varkey E, McCrory DC, Pedersen SA, Linde M. Biofeedback as prophylaxis for pediatric migraine: a meta-analysis. Pediatrics 2016 Aug;138(2) [FREE Full text] [doi: 10.1542/peds.2016-0675] [Medline: 27462067]
11. Nestoriuc Y, Martin A. Efficacy of biofeedback for migraine: a meta-analysis. Pain 2007 Mar;128(1-2):111-127. [doi: 10.1016/j.pain.2006.09.007] [Medline: 17084028]
12. Andrasik F. Behavioral treatment of headaches: extending the reach. Neurol Sci 2012 May;33 Suppl 1:S127-S130. [doi: 10.1007/s10072-012-1073-2] [Medline: 22644187]
13. Schwartz MS, Andrasik F, editors. Biofeedback: A Practitioner's Guide. New York City: Guilford Press; 2017.
14. Minen MT, Torous J, Raynowska J, Piazza A, Grudzen C, Powers S, et al. Electronic behavioral interventions for headache: a systematic review. J Headache Pain 2016;17:51 [FREE Full text] [doi: 10.1186/s10194-016-0608-y] [Medline: 27160107]
15. Luxton DD, McCann RA, Mishkind MC, Reger GM, Bush NE. mHealth for mental health: integrating smartphone technology in behavioral healthcare. Prof Psychol Res Pr 2011;42(6):505-512 [FREE Full text] [doi: 10.1037/a0024485]
16. Constantinescu G, Loewen I, King B, Hodgetts W, Rieger J, Brodt C. Designing a mobile health app for patients with dysphagia following head and neck cancer: a qualitative study. JMIR Rehabil Assist Technol 2017;4(1):e3. [Medline: 28582245]
17. O'Reilly M, Duffin J, Ward T, Caulfield B. Mobile app to streamline the development of wearable sensor-based exercise biofeedback systems: system development and evaluation. JMIR Rehabil Assist Technol 2017;4(2):e9. [doi: 10.2196/rehab.7259]
18. Kottner J, Audige L, Brorson S, Donner A, Gajewski BJ, Hróbjartsson A, et al. Guidelines for reporting reliability and agreement studies (GRRAS) were proposed. Int J Nurs Stud 2011 Jun;48(6):661-671. [doi: 10.1016/j.ijnurstu.2011.01.016] [Medline: 21514934]
19. Larman C, Basili VR. Iterative and incremental developments: a brief history. Comput 2003;36(6):47-56. [doi: 10.1109/MC.2003.1204375]
20. Bonett DG. Sample size requirements for estimating intraclass correlations with desired precision. Stat Med 2002 May 15;21(9):1331-1335. [doi: 10.1002/sim.1108] [Medline: 12111881]
21. Hermens HJ, Freriks B, Disselhorst-Klug C, Rau G. Development of recommendations for SEMG sensors and sensor placement procedures. J Electromyogr Kinesiol 2000 Oct;10(5):361-374. [Medline: 11018445]
22. Criswell E. Cram's Introduction to Surface Electromyography. 2nd edition. Sudbury, MA: Jones & Bartlett Publishers; 2010.
23. Mathiassen SE, Winkel J, Hägg GM. Normalization of surface EMG amplitude from the upper trapezius muscle in ergonomic studies - A review. J Electromyogr Kinesiol 1995 Dec;5(4):197-226. [Medline: 20719652]
24. Burden A. How should we normalize electromyograms obtained from healthy participants? What we have learned from over 25 years of research. J Electromyogr Kinesiol 2010 Dec;20(6):1023-1035. [doi: 10.1016/j.jelekin.2010.07.004] [Medline: 20702112]
25. Knutson LM, Soderberg GL, Ballantyne BT, Clarke WR. A study of various normalization procedures for within day electromyographic data. J Electromyogr Kinesiol 1994;4(1):47-59. [doi: 10.1016/1050-6411(94)90026-4] [Medline: 20870546]
26. Chowdhury RH, Reaz MB, Ali MA, Bakar AA, Chellappan K, Chang TG. Surface electromyography signal processing and classification techniques. Sensors (Basel) 2013 Sep 17;13(9):12431-12466 [FREE Full text] [doi: 10.3390/s130912431] [Medline: 24048337]
27. Bland JM, Altman DG. Statistical methods for assessing agreement between two methods of clinical measurement. Lancet 1986 Feb 8;1(8476):307-310. [Medline: 2868172]
28. Shrout PE, Fleiss JL. Intraclass correlations: uses in assessing rater reliability. Psychol Bull 1979 Mar;86(2):420-428. [Medline: 18839484]
29. Watson PF, Petrie A. Method agreement analysis: a review of correct methodology. Theriogenology 2010 Jun;73(9):1167-1179 [FREE Full text] [doi: 10.1016/j.theriogenology.2010.01.003] [Medline: 20138353]
30. Barnhart HX, Haber MJ, Lin LI. An overview on assessing agreement with continuous measurements. J Biopharm Stat 2007;17(4):529-569. [doi: 10.1080/10543400701376480] [Medline: 17613641]

31. Cicchetti DV. Guidelines, criteria, and rules of thumb for evaluating normed and standardized assessment instruments in psychology. Psychol Assess 1994;6(4):284-290. [doi: 10.1037/1040-3590.6.4.284]
32. Schmidt B. Proof of Principle studies. Epilepsy Res 2006 Jan;68(1):48-52. [doi: 10.1016/j.eplepsyres.2005.09.019] [Medline: 16377153]
33. Sarafino EP, Goehring P. Age comparisons in acquiring biofeedback control and success in reducing headache pain. Ann Behav Med 2000;22(1):10-16. [Medline: 10892524]
34. Bergmann JH, McGregor AH. Body-worn sensor design: what do patients and clinicians want? Ann Biomed Eng 2011 Sep;39(9):2299-2312. [doi: 10.1007/s10439-011-0339-9] [Medline: 21674260]
35. Fleiss JL. Design and Analysis of Clinical Experiments. Hoboken, NJ: John Wiley & Sons; 2011.
36. Walter SD, Eliasziw M, Donner A. Sample size and optimal designs for reliability studies. Stat Med 1998 Jan 15;17(1):101-110. [Medline: 9463853]
37. Merletti R, di Torino P. Standards for reporting EMG data. J. Electromyogr Kinesiol 1999;9(1):3-4 [FREE Full text]
38. Kelechi TJ, Michel Y, Wiseman J. Are infrared and thermistor thermometers interchangeable for measuring localized skin temperature? J Nurs Meas 2006;14(1):19-30. [Medline: 16764175]
39. Ives JC, Wigglesworth JK. Sampling rate effects on surface EMG timing and amplitude measures. Clin Biomech (Bristol, Avon) 2003 Jul;18(6):543-552. [Medline: 12828904]
40. Durkin JL, Callaghan JP. Effects of minimum sampling rate and signal reconstruction on surface electromyographic signals. J Electromyogr Kinesiol 2005 Oct;15(5):474-481. [doi: 10.1016/j.jelekin.2005.02.003] [Medline: 15935959]
41. van Boxtel A. Optimal signal bandwidth for the recording of surface EMG activity of facial, jaw, oral, and neck muscles. Psychophysiol 2001 Jan;38(1):22-34. [Medline: 11321618]
42. De Luca CJ, Gilmore LD, Kuznetsov M, Roy SH. Filtering the surface EMG signal: movement artifact and baseline noise contamination. J Biomech 2010 May 28;43(8):1573-1579. [doi: 10.1016/j.jbiomech.2010.01.027] [Medline: 20206934]
43. Müller R, Büttner P. A critical discussion of intraclass correlation coefficients. Stat Med 1994;13(23-24):2465-2476. [Medline: 7701147]
44. McGraw KO, Wong SP. Forming inferences about some intraclass correlation coefficients. Psychol Methods 1996;1(1):30-46. [doi: 10.1037/1082-989X.1.1.30]
45. Bartko JJ. The intraclass correlation coefficient as a measure of reliability. Psychol Rep 1966 Aug;19(1):3-11. [doi: 10.2466/pr0.1966.19.1.3] [Medline: 5942109]
46. Bland JM, Altman DG. Measuring agreement in method comparison studies. Stat Methods Med Res 1999 Jun;8(2):135-160. [Medline: 10501650]
47. Bland JM, Altman DG. A note on the use of the intraclass correlation coefficient in the evaluation of agreement between two methods of measurement. Comput Biol Med 1990;20(5):337-340. [Medline: 2257734]
48. Clancy EA, Farry KA. Adaptive whitening of the electromyogram to improve amplitude estimation. IEEE Trans Biomed Eng 2000 Jun;47(6):709-719. [doi: 10.1109/10.844217] [Medline: 10833845]
49. Rausa M, Palomba D, Cevoli S, Lazzerini L, Sancisi E, Cortelli P, et al. Biofeedback in the prophylactic treatment of medication overuse headache: a pilot randomized controlled trial. J Headache Pain 2016 Dec;17(1):87 [FREE Full text] [doi: 10.1186/s10194-016-0679-9] [Medline: 27655371]
50. Rains JC. Change mechanisms in EMG biofeedback training: cognitive changes underlying improvements in tension headache. Headache 2008 May;48(5):735-6; discussion 736. [doi: 10.1111/j.1526-4610.2008.01119_1.x] [Medline: 18471128]
51. Munster-Segev M, Fuerst O, Kaplan SA, Chan A. Incorporation of a stress reducing mobile app in the care of patients with type 2 diabetes: a prospective study. JMIR mHealth and uHealth 2017;5(5):e75. [Medline: 28554881]
52. Uddin AA, Morita PP, Tallevi K, Armour K, Li J, Nolan RP, et al. Development of a wearable cardiac monitoring system for behavioral neurocardiac training: a usability study. JMIR Mhealth Uhealth 2016;4(2):e45 [FREE Full text] [doi: 10.2196/mhealth.5288] [Medline: 27106171]
53. Dooley EE, Golaszewski NM, Bartholomew JB. Estimating accuracy at exercise intensities: a comparative study of self-monitoring heart rate and physical activity wearable devices. JMIR mHealth and uHealth 2017;5(3):e34. [Medline: 28302596]

Abbreviations

CCC: concordance correlation coefficient
ECG: electrocardiogram
ICC: intraclass correlation coefficient
LOA: limits of agreement
MD: mean difference
mHealth: mobile health
MVC: maximal voluntary contraction
MVP: minimal viable product

RMS: root mean square
SEMG: surface electromyography
VC50: voluntary contraction at 50% force
VC25: voluntary contraction at 25% force
WHMS: wearable health monitoring sensors

Edited by G Eysenbach; submitted 28.09.17; peer-reviewed by M Minen, YCP Arai; comments to author 09.12.17; revised version received 21.01.18; accepted 23.01.18; published 23.02.18.

Please cite as:
Stubberud A, Omland PM, Tronvik E, Olsen A, Sand T, Linde M
Wireless Surface Electromyography and Skin Temperature Sensors for Biofeedback Treatment of Headache: Validation Study with Stationary Control Equipment
JMIR Biomed Eng 2018;3(1):e1
URL: http://biomedeng.jmir.org/2018/1/e1/
doi:10.2196/biomedeng.9062
PMID:

Original Paper

Auralife Instant Blood Pressure App in Measuring Resting Heart Rate: Validation Study

Timothy B Plante[1], MD, MHS; Anna C O'Kelly[2], MD, MPhil; Bruno Urrea[3], MD; Zane T Macfarlane[4], BA; Lawrence J Appel[5], MD, MPH; Edgar R Miller III[5], MD, PhD; Roger S Blumenthal[6], MD; Seth S Martin[5,6,7], MD, MHS

[1]Department of Medicine, Larner College of Medicine, University of Vermont, Colchester, VT, United States

[2]Department of Medicine, Massachusetts General Hospital, Boston, MA, United States

[3]Department of Medicine, MedStar Health Union Memorial Hospital, Baltimore, MD, United States

[4]Department of Chemistry, Pomona College, Claremont, CA, United States

[5]Johns Hopkins University, Welch Center for Prevention, Epidemiology, and Clinical Research, Baltimore, MD, United States

[6]Ciccarone Center for the Prevention of Cardiovascular Disease, Johns Hopkins University School of Medicine, Baltimore, MD, United States

[7]Malone Center for Engineering in Healthcare, Johns Hopkins University Whiting School of Engineering, Baltimore, MD, United States

Corresponding Author:
Timothy B Plante, MD, MHS
Department of Medicine
Larner College of Medicine
University of Vermont
360 S Park Drive
Room 206B
Colchester, VT, 05446
United States
Phone: 1 8026563688
Fax: 1 8026568965
Email: timothy.plante@uvm.edu

Abstract

Background: mHealth apps that measure heart rate using pulse photoplethysmography (PPG) are classified as class II (moderate-risk) Food and Drug Administration devices; therefore, these devices need clinical validation prior to public release. The Auralife Instant Blood Pressure app (AuraLife IBP app) is an mHealth app that measures blood pressure inaccurately based on a previous validation study. Its ability to measure heart rate has not been previously reported.

Objective: The objective of our study was to assess the accuracy and precision of the AuraLife IBP app in measuring heart rate.

Methods: We enrolled 85 adults from ambulatory clinics. Two measurements were obtained using the AuraLife IBP app, and 2 other measurements were achieved with a oscillometric device. The order of devices was randomized. Accuracy was assessed by calculating the relative and absolute mean differences between heart rate measurements obtained using each AuraLife IBP app and an average of both standard heart rate measurements. Precision was assessed by calculating the relative and absolute mean differences between individual measurements in the pair for each device.

Results: The relative and absolute mean (SD) differences between the devices were 1.1 (3.5) and 2.8 (2.4) beats per minute (BPM), respectively. Meanwhile, the within-device relative and absolute mean differences, respectively, were <0.1 (2.2) and 1.7 (1.4) BPM for the standard device and −0.1 (3.2) and 2.2 (2.3) BPM for the AuraLife IBP app.

Conclusions: The AuraLife IBP app had a high degree of accuracy and precision in the measurement of heart rate. This supports the use of PPG technology in smartphones for monitoring resting heart rate.

(JMIR Biomed Eng 2018;3(1):e11057) doi:10.2196/11057

KEYWORDS

mHealth; digital health; heart rate; validation study; photoplethysmography; medical informatics; mobile phones

Introduction

Pulse photoplethysmograms (PPGs) quantify circulation-related color changes in the vascular beds using optical sensors, and it can be used to measure heart rate [1]. Heart rate monitors use PPG are class II (moderate risk) Food and Drug Administration devices, and these devices must undergo clinical validation prior to their release [2]. Several consumer apps leverage the built-in camera and light to obtain PPG-measured heart rate from an illuminated body part (eg, finger). Most of these apps accurately measure heart rate compared with a standard device [3-5].

The Instant Blood Pressure (IBP) app (AuraLife IBP app, AuraLife, Newport Beach, CA) is an mHealth app that measures blood pressure and heart rate using a smartphone with no additional sensors. Both measurements are presented simultaneously to the user. The app sold >148,000 copies and earned >US $600,000 in revenue within 13 months after its availability [6-8]. It was removed from the app store for unclear reasons in July 2015. We previously reported the inaccuracy of the AuraLife IBP app in measuring blood pressure compared with a validated oscillometric device. Moreover, its measurement process incorporated user-entered demographic and anthropomorphic data in determining blood pressure [6,9,10]. In multiple linear regression modeling of predicted systolic and diastolic blood pressure on user-entered data, sex, age, height, and weight of the participants accounted for only 12% and 12% of the variance in systolic and diastolic blood pressure results for the standard device, respectively, but 66% and 82% of the variability of these measurements for the AuraLife IBP app. The manufacturers of the AuraLife IBP app have raised concerns about our validation protocol and suggested that our findings could be because of hemodynamic changes resulting from the specific protocol [10,11]. These hemodynamic changes would also affect heart rate. However, the precision and accuracy of the app in measuring heart rate have not been reported.

Determining the accuracy and precision of the AuraLife IBP app in measuring heart rate would provide valuable information for those using the AuraLife IBP app for this purpose and its technology in general. More importantly, this report would provide insight about the quality of the overall validation protocol that we used. The high levels of accuracy and precision of the AuraLife IBP app would support the quality of the overall assessment protocol and confirm the inaccuracy of the blood pressure measurement. Low accuracy or precision in obtaining heart rate could be due to protocol-related hemodynamic changes in patients (too much movement), not enough time between measurements, or app-related performance characteristics, and these would support the manufacturer's concerns. Finally, it provides the opportunity to determine if the heart rate measurement was also inappropriately dependent on user-entered variables. Herein, we report the accuracy and precision metrics of the AuraLife IBP app in measuring heart rate and the variability of heart rate measurements accounted for by user-entered demographic and anthropomorphic data.

Methods

Validation Protocol

The methods of this validation protocol have been published elsewhere [6]. We prescreened participants aged ≥18 years for enrollment who were referred from 4 ambulatory clinics at Johns Hopkins University School of Medicine and an ambulatory research site. We excluded participants with contraindications to blood pressure measurement in both arms, internal devices (eg, pacemaker), active arrhythmias, height or weight values outside of the supported range by the AuraLife IBP app (height: <42 or >84 in and weight: <65 or >450 lbs), missing fingers, or inability to follow instructions. Prespecified rules have stated that participants with sequential systolic blood pressure measurements of >12 mmHg or diastolic blood pressure measurements of >8 mmHg (based on international validation guidelines [12]) will be dropped out from the study.

The participants self-reported date of birth, sex, height, weight, race, ethnicity, highest level of education, history of hypertension, and receipt of antihypertensive medications. The research staff recorded the patient's date of birth, sex, height, and weight into the app. The participants underwent 5 minutes of quiet sitting. Then, they had 2 pairs of blood pressure and heart rate measurements obtained from each device, of which the sequence was random. The standard devices used were the Omron 907 or Omron 907XL oscillometric noninvasive blood pressure and heart rate monitors, which had an heart rate measurement range of 30 to 199 BPM and an heart rate accuracy within 5% of the reading [13]. These devices were calibrated prior to the enrollment of the first participant. We used the AuraLife IBP app version 1.2.3 installed on an iPhone 5s and iPhone 6 running iOS version 8.3 (Apple Inc, Cupertino, CA), which has a reported heart rate measurement ranging from 39 to 240 BPM [14]. Measurements from the AuraLife IBP app and the standard device were separated by 60 seconds.

Accuracy

In accuracy analyses, we compared each individual heart rate measurement obtained using the AuraLife IBP app with the standard heart rate measurement, which was a mean of the heart rate measurements obtained using both standard devices. We calculated the mean relative difference and mean absolute difference between the AuraLife IBP app and standard equipment. Accuracy was visualized with scatterplot and Bland-Altman plot using a short dashed gray line to indicate the mean relative difference of the AuraLife IBP app minus standard and long dashed gray lines to indicate 2 SD.

Precision

For precision metrics, we subtracted the second app measurement from the first app measurement, calculating the mean relative difference and mean absolute difference between successive measurements for the same device. This was also performed for the standard device. Precision was visualized with paired coordinate plots. A black dashed line connected the mean of each reading for each device.

Dependence on User-Entered Variables

To assess the possibility of dependence of user-entered variables on heart rate obtained using the AuraLife IBP app, we repeated the same regressions that have been previously described [10], that is, we regressed the reported heart rate for the standard device and AuraLife IBP app on the age at the date of study enrollment, gender (male), height in inches, and weight in pounds. We interpreted the correlating R^2 as the percentage of the dependent variable (heart rate from each device) explained by the independent variables. We compared R^2 values of the AuraLife IBP app and those of the standard device. This study was approved by the institutional review board of the Johns Hopkins University School of Medicine. All analyses were performed with Stata MP 14.2 (StataCorp, College Station, TX).

Results

Validation Protocol

In August 2015 and September 2015, we prescreened 105 individuals, of whom 4 did not meet the inclusion criteria of the study (active atrial fibrillation, n=1, or the presence of a pacemaker, n=3). Of the 101 enrolled patients, 3 were not included owing to standard device errors, and 13 were excluded owing to high variation in successive standard device systolic blood pressure measurements (n=7), diastolic blood pressure measurements (n=4), or both (n=2). We were unable to obtain blood pressure and heart rate results for 23 of the attempted 170 AuraLife IBP app measurements because the app encountered an error and was unable to produce a measurement. These were missing from the first pair in 5 individuals (n=5 measurements), the second pair in 4 individuals (n=4 measurements), and both pairs in 7 individuals (n=14 measurements). The complete pairs of the AuraLife IBP app measurements were obtained in 69 individuals.

The mean (SD) age of the participants was 57 (16) years. Of these participants, 48% (41/85) were men. Moreover, 61% (52/85) were white, 28% (24/85) were black, and 9% (8/85) were Asian (Table 1). The range of the heart rate measurements obtained using the standard device was 46 to 94 BPM for the first measurement, 45 to 94 BPM for the second measurement, and 46 to 94 BPM for the standard measurement (mean of both measurements used in the accuracy analysis). The range of the measurements obtained using the AuraLife IBP app was 46 to 96 BPM for the first measurement and 45 to 99 BPM for the second measurement.

Accuracy

The mean relative difference for heart rate obtained using the AuraLife IBP app and standard device was 1.1 (3.5) BPM. The mean absolute difference was 2.8 (2.4) BPM (Table 2). The scatterplot showed a high correlation for heart rate measurements obtained using the AuraLife IBP app and standard devices with Pearson r=0.95 (P<.001), as seen in Figure 1. The Bland-Altman plot showed a nondifferential pattern across the means, as seen in Figure 2, with the dotted line indicating the mean and dashed lines representing 2 SD.

Table 1. Baseline characteristics.

Demographics	Participants (n=85)	Range
Age (years), mean (SD)	57 (16)	18-81
Male, n (%)	41 (48)	
White, n (%)	52 (61)	
Black, n (%)	24 (28)	
Asian, n (%)	8 (9)	
Hispanic ethnicity, n (%)	4 (5)	
Body mass index (kg/m^2), mean (SD)	28 (6)	18-51
Standard systolic blood pressure (mm Hg), mean (SD)	126 (17)	92-170
Standard diastolic blood pressure (mm Hg), mean (SD)	70 (11)	32-100
Standard heart rate (beats per minute), mean (SD)	68 (11)	46-94
Hypertension, n (%)	45 (53)	
On medication, n (%)	41 (91)	
Owns a smartphone, n (%)	71 (84)	

Table 2. Mean difference between devices.

Difference (beats per minute)	Mean (SD) difference	Range
Relative	1.1 (3.5)	−9 to 12
Absolute	2.8 (2.4)	0 to 12

Figure 1. Accuracy visualization: Scatterplot of AuraLife Instant Blood Pressure (IBP) app heart rate measurements versus the standard heart rate measurements. BPM: beats per minute.

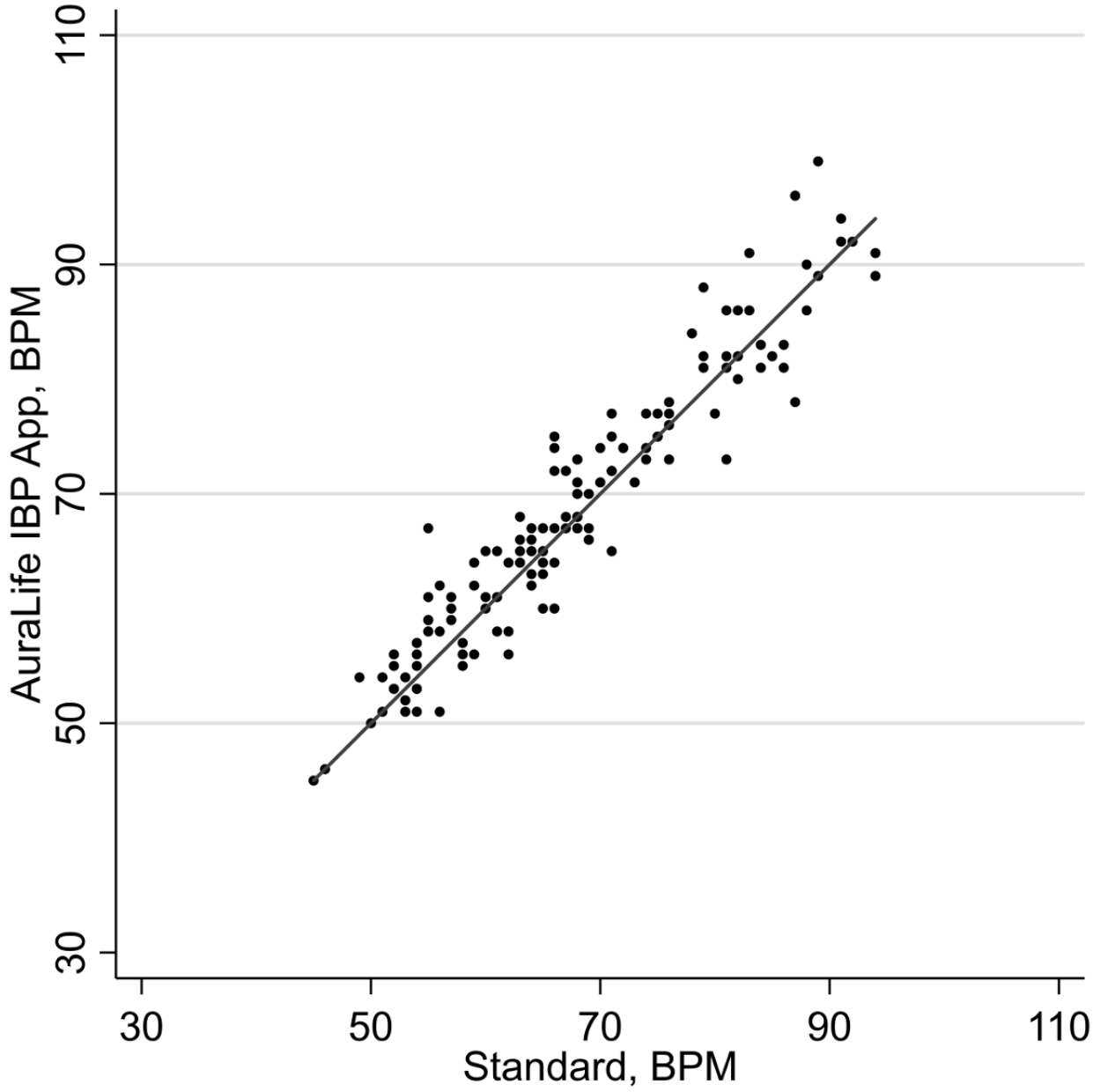

Figure 2. Accuracy visualization: Bland-Altman plot for the AuraLife Instant Blood Pressure (IBP) app heart rate measurements and the standard measurements. BPM: beats per minute.

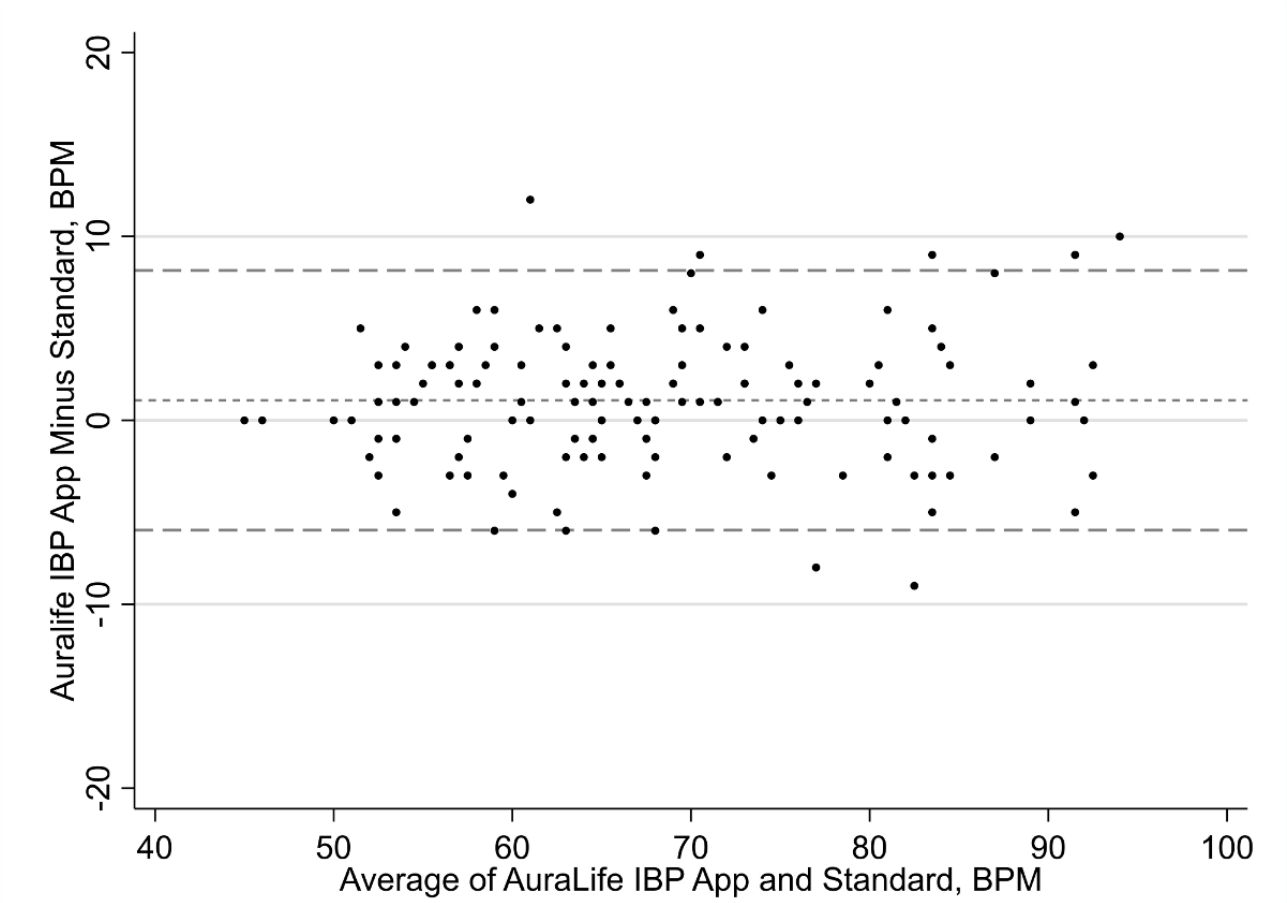

Table 3. Precision metrics for each device.

Device	Mean (SD) difference	Range
Standard device (n=85)		
Relative, beats per minute	0.01 (2.2)	−6 to 5
Absolute, beats per minute	1.7 (1.4)	0 to 6
AuraLife IBP App (n=69)		
Relative, beats per minute	−0.1 (3.2)	−13 to 7
Absolute, beats per minute	2.2 (2.3)	0 to 13

Precision

For the AuraLife IBP app, the mean relative difference between the 69 pairs of measurements was −0.1 (3.2) BPM, whereas the mean absolute difference was 2.2 (2.3) BPM (Table 3). For the standard device, the mean relative difference between the 85 pairs of measurements was 0.01 (2.2) BPM. Meanwhile, the mean absolute difference was 1.7 (1.4) BPM. The paired coordinate plot showed minimal variability between the first and second measurements from each device, as seen in Figure 3, with dashed lines representing mean values.

Dependence on User-Entered Variables

The regression of user-entered demographic and anthropomorphic data on the reported heart rate obtained similar R^2 values for the standard device and the AuraLife IBP app (Table 4). The independent variables accounted for 19% and 16% of the heart rate variability for the standard device and AuraLife IBP app, respectively.

Figure 3. Precision visualization: Paired coordinate plot for AuraLife Instant Blood Pressure (IBP) app and the standard device. BPM: beats per minute; HR: heart rate.

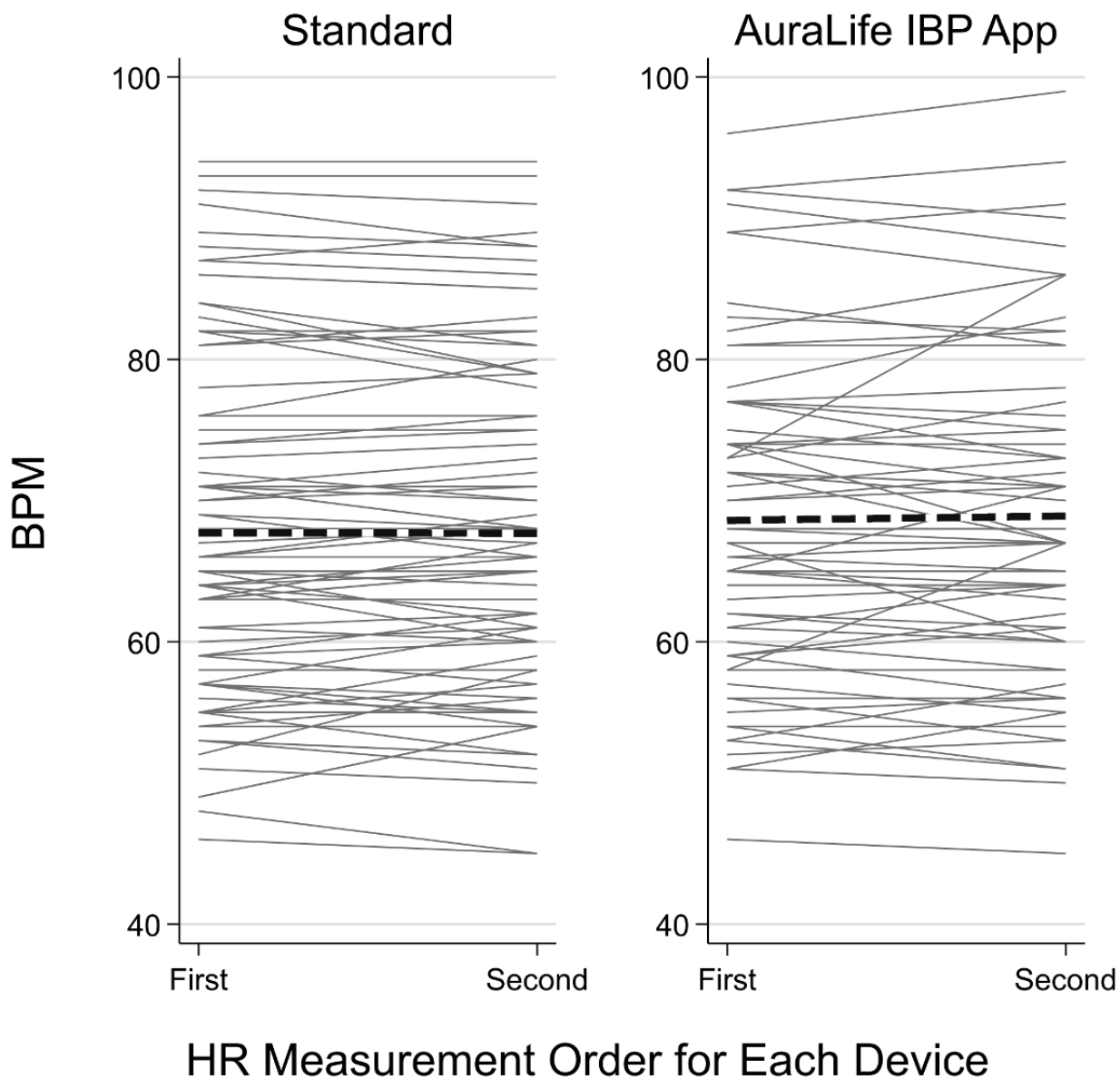

Table 4. Regression coefficients.

Device	Regression coefficients					
	Age (years)	Male	Height (inches)	Weight (lbs)	Constant	R^2
Standard heart rate	−0.24	−5.74	−0.04	0.07	74.68	0.19
AuraLife Instant Blood Pressure app heart rate	−0.23	−5.73	0.05	0.05	73.11	0.16

Discussion

Principal Findings

In this validation study of heart rate measurements obtained using an mHealth app that was previously found to be inaccurate in measuring blood pressure, we revealed that the AuraLife IBP app has a high degree of accuracy and precision for the measurement of heart rate. The heart rate measurement had a similar amount of demographic or anthropomorphic information as the standard device, which is minimal.

Implications

Prior assessments of heart rate measuring-devices have generally been positive, and one meta-analysis has reported a pooled correlation coefficient of 0.95 [15], which is identical to that

observed in this validation protocol. The use of these apps for the detection of heart rate in the context of arrhythmia is limited. Unfortunately, our protocol intentionally excluded participants with arrhythmias because the standard device is not validated to obtain heart rate or blood pressure measurements in individuals with arrhythmias.

The accuracy of the heart rate measurements with the AuraLife IBP app provides reassurance that our study protocol did not induce hemodynamic changes, which could have potentially biased the results of our blood pressure validation study. This was a concern raised by the app developers. Hence, results from this validation study of heart rate provide an indirect support to our previous blood pressure validation study about the AuraLife IBP app. Therefore, our protocol may be useful for other researchers interested in comparing the performance characteristics of mHealth apps with those of a validated oscillometric device.

Limitations

Because the protocol was primarily designed as a blood pressure validation study, all measurements were obtained at rest and had limited range. Whether the accuracy or precision of the AuraLife IBP app in measuring heart rate will change with exercise or for individuals with resting values at greater extremes is unclear. We did not include individuals with arrhythmias. Thus, whether the performance metrics will be similar among these patients is unclear. Although the standard device is widely used in clinical practice for measuring heart rate and blood pressure, it is not a conventional standard for heart rate or blood pressure measurement in clinical studies. Future studies that use a more conventional method, such as electrocardiography, or those that include trained observers who will use a random-zero sphygmomanometer must be conducted. Finally, we did not test the Android version of the app.

Conclusions

The AuraLife IBP app has high accuracy and precision in measuring heart rate in adult ambulatory patients. This further supports the use of PPG technology in smartphones for monitoring resting heart rate.

Acknowledgments

We thank Jeanne Charleston, PhD BSN for her assistance in providing training and standard device management; Morgan Grams, MD PhD MHS, Satish Misra, MD, and Haitham Ahmed, MD in their assistance in trial design. We thank the clinical staff at the Johns Hopkins General Internal Medicine, Cardiology, Nephrology, and ProHealth sites for assistance in study execution. We thank the Johns Hopkins legal team for guidance on interactions with AuraLife. This study was supported by the PJ Schafer Cardiovascular Research Grant. TBP was funded by the Institutional National Research Service Awards from the Health Resources and Services Administration (T32HP10025B0) and the National Heart, Lung, and Blood Institute (2T32HL007180-41A1).

Conflicts of Interest

SSM reports research support from Google, Apple, Nokia, iHealth, and the Aetna Foundation. There are no other relevant conflicts of interest.

References

1. Elgendi M. On the analysis of fingertip photoplethysmogram signals. Curr Cardiol Rev 2012 Feb;8(1):14-25 [FREE Full text] [Medline: 22845812]
2. US Food & Drug Administration. Cardiac Monitor Guidance (including Cardiotachometer and Rate Alarm) - Guidance for Industry URL: https://www.fda.gov/MedicalDevices/ucm073940.htm [accessed 2018-05-15] [WebCite Cache ID 6zRGjyIEW]
3. Mitchell K, Graff M, Hedt C, Simmons J. Reliability and validity of a smartphone pulse rate application for the assessment of resting and elevated pulse rate. Physiother Theory Pract 2016 Aug;32(6):494-499. [doi: 10.1080/09593985.2016.1203046] [Medline: 27459148]
4. Yan BP, Chan CK, Li CK, To OT, Lai WH, Tse G, et al. Resting and Postexercise Heart Rate Detection From Fingertip and Facial Photoplethysmography Using a Smartphone Camera: A Validation Study. JMIR Mhealth Uhealth 2017 Mar 13;5(3):e33 [FREE Full text] [doi: 10.2196/mhealth.7275] [Medline: 28288955]
5. Poh M, Poh YC. Validation of a Standalone Smartphone Application for Measuring Heart Rate Using Imaging Photoplethysmography. Telemed J E Health 2017 Aug;23(8):678-683. [doi: 10.1089/tmj.2016.0230] [Medline: 28140834]
6. Plante TB, Urrea B, MacFarlane ZT, Blumenthal RS, Miller III ER, Appel LJ, et al. Validation of the Instant Blood Pressure Smartphone App. JAMA Intern Med 2016 May 01;176(5):700-702. [doi: 10.1001/jamainternmed.2016.0157] [Medline: 26938174]
7. Federal Trade Commission. Marketers of Blood-Pressure App Settle FTC Charges Regarding Accuracy of App Readings URL: https://www.ftc.gov/news-events/press-releases/2016/12/marketers-blood-pressure-app-settle-ftc-charges-regarding [accessed 2018-05-15] [WebCite Cache ID 6zRGqDyap]

8. Plante TB, O'Kelly AC, Macfarlane ZT, Urrea B, Appel LJ, Miller III ER, et al. Trends in user ratings and reviews of a popular yet inaccurate blood pressure-measuring smartphone app. J Am Med Inform Assoc 2018 Aug 01;25(8):1074-1079. [doi: 10.1093/jamia/ocy060] [Medline: 29878236]
9. El Assaad MA, Topouchian J, Darné BM, Asmar RG. Validation of the Omron HEM-907 device for blood pressure measurement. Blood Press Monit 2002 Aug;7(4):237-241. [Medline: 12198340]
10. Plante TB, Appel LJ, Martin SS. Critical Flaws in the Validation of the Instant Blood Pressure Smartphone App-A Letter from the App Developers-Reply. JAMA Intern Med 2016 Sep 01;176(9):1410-1411. [doi: 10.1001/jamainternmed.2016.4765] [Medline: 27598762]
11. Archdeacon R, Schneider R, Jiang Y. Critical Flaws in the Validation of the Instant Blood Pressure Smartphone App-A Letter From the App Developers. JAMA Intern Med 2016 Dec 01;176(9):1410. [doi: 10.1001/jamainternmed.2016.4753] [Medline: 27598761]
12. Graves J, Quinn D. ISO 81060-2:2013. Non-invasive sphygmomanometers - Part 2: Clinical investigation of automated measurement type. ANSI/AAMI/ISO; 2013.
13. HEM-907XL Professional Digital Blood Pressure Monitor. Omron Healthcare Wellness & Healthcare Products URL: https://omronhealthcare.com/wp-content/uploads/hem-907xl_product_guide1.pdf [accessed 2018-07-05] [WebCite Cache ID 70gujO22h]
14. Instant Blood Pressure Website. 2016. The App URL: https://web.archive.org/web/20160201161554/http://www.instantbloodpressure.com/the-app/ [accessed 2018-07-06] [WebCite Cache ID 70iEiTgKP]
15. De Ridder B, Van Rompaey B, Kampen JK, Haine S, Dilles T. Smartphone Apps Using Photoplethysmography for Heart Rate Monitoring: Meta-Analysis. JMIR Cardio 2018 Feb 27;2(1):e4. [doi: 10.2196/cardio.8802]

Abbreviations

BPM: beats per minute
IBP: Instant Blood Pressure
PPG: pulse photoplethysmogram

Edited by G Eysenbach; submitted 15.05.18; peer-reviewed by J Goris, S Omboni; comments to author 21.06.18; revised version received 06.07.18; accepted 23.07.18; published 21.11.18.

Please cite as:
Plante TB, O'Kelly AC, Urrea B, Macfarlane ZT, Appel LJ, Miller III ER, Blumenthal RS, Martin SS
Auralife Instant Blood Pressure App in Measuring Resting Heart Rate: Validation Study
JMIR Biomed Eng 2018;3(1):e11057
URL: http://biomedeng.jmir.org/2018/1/e11057/
doi:10.2196/11057
PMID:

Original Paper

Relationship Between the Applied Occlusal Load and the Size of Markings Produced Due to Occlusal Contact Using Dental Articulating Paper and T-Scan: Comparative Study

Shravya Reddy[1*], BDS, MDS; Preeti S Kumar[1*], BDS, MDS; Vyoma V Grandhi[1*], BDS, MDS

Department of Prosthodontics, The Oxford Dental College, Bangalore, India

[*]all authors contributed equally

Corresponding Author:
Preeti S Kumar, BDS, MDS
Department of Prosthodontics
The Oxford Dental College
10th Mile Stone, Hosur Road, Bommanahalli
Bangalore, 560065
India
Phone: 91 9845493230
Email: drpreetisatheesh@gmail.com

Abstract

Background: The proposed experimental design was devised to determine whether a relationship exists between the occlusal load applied and the size of the markings produced from tooth contact when dental articulating paper and T-Scan are interposed alternatively.

Objective: The objective of our study was to compare the relationship between contact markings on an articulating paper and T-Scan for an applied occlusal load.

Methods: In this in vitro study, dentulous maxillary and mandibular dies were mounted on a metal jig and articulating paper and T-Scan sensor were placed alternatively between the casts. Loads simulating occlusal loads began at 25 N and incrementally continued up to 450 N. The resultant markings (180 marks resulting from articulating paper and 138 from T-Scan) were photographed, and the marks were analyzed using MOTIC image analysis and sketching software. Descriptive statistical analyses were performed using one-way analysis of variance, Student *t* test, and Pearson correlation coefficient method.

Results: Statistical interpretation of the data indicated that with articulating paper, the mark area increased nonlinearly with increasing load and there was a false-positive result. The characteristics of the paper mark appearance did not describe the amount of occlusal load present on a given tooth. The contact marking obtained using T-Scan for an applied occlusal load indicated that the mark area increased with increase in the load and provided more predictable results of actual load content within the occlusal contact.

Conclusions: The size of an articulating paper mark may not be a reliable predictor of the actual load content within the occlusal contact, whereas a T-Scan provides more predictable results of the actual load content within the occlusal contact.

(JMIR Biomed Eng 2018;3(1):e11347) doi:10.2196/11347

KEYWORDS

occlusal indicator; occlusal load; articulating paper; T-Scan

Introduction

Over the years, occlusal analysis has been a matter of guesswork. Occlusal indicators are widely used in dental treatment to measure tooth contacts that occur during occlusion. They are important tools in locating interference and refining occlusal contacts during prosthodontic rehabilitation [1]. Aids such as articulating paper, waxes, and pressure-indicating paste are used when a dentist has to assess and balance the occlusal forces. The accurate measurement of tooth contacts can provide valuable information for diagnostic, treatment, or prognostic purposes. Hence, the accuracy of these indicators is essential for the establishment of occlusal harmony [2].

Occlusal indicators can be broadly divided into two categories based on their measurement capacity: qualitative and

quantitative indicators. Qualitative indicators, such as the articulating paper and articulating silk, are limited in measurement to only the location and number of tooth contacts [1]; these are the most commonly used indicators because of their low cost and ease of application. Quantitative indicators, on the other hand, include electro-optic and resistive techniques such as the T-Scan pressure measurement system; these indicators have the added capability of measuring the time and force characteristics of tooth contacts, but they are more expensive [1].

It has been advocated in textbooks on occlusion [3-8] that the articulating paper mark area is a representative of the load contained within the mark. While using the articulating paper, we tend to assume that a vivid occlusal contact is the location where a large occlusal force has been applied [9]. The articulating paper mark appearance describes that large and dark marks indicate heavy load, whereas smaller and light marks indicate lightloads. Additionally, the presence of many similar-sized marks spread around the contacting arches is purported to indicate the equal occlusal contact intensity, evenness, and simultaneity [10]. However, limited literature exists to clinically correlate and confirm these findings. By employing articulating paper as a force measurement device, we, as clinicians, miss properly seeing the occlusal force, occlusal contact intensity, evenness, and simultaneity [9]. Hence, this proposed experimental design was devised to determine whether a relationship exists between the applied occlusal load and the size of the markings produced from the tooth contact when a clinically used dental articulating paper and T-scan are interposed alternatively.

Methods

Materials Used

We used Bausch 40-µm microthin articulating papers and ultrathin T-Scan III sensor (.004 inch, 0.1 mm). The articulating paper was tear resistant and coated with liquid colors on both sides. The special color coating with liquid colors consists of many color-filled microcapsules. Even the slightest masticatory pressure can cause the capsules to burst and, thus, release the distinctly visible color. The T-Scan system comprises a sensor, handle and cable, system unit, and software that detect patients' occlusal forces. The handle's attached USB cable is then connected directly to the computer via the USB port.

Mounting of Metal Dies and Contact Procedure

Using articulating paper mark, occlusal loads were evaluated on a solid metal die (Figure 1) with no soft-tissue components. Vertical loading was accomplished by designing a cast anchoring apparatus that attached the metal dies to a metal jig. The metal dies were secured to the metal jig through machined rods with alignment holes (Figure 2) that ensured a precise alignment of the maxillary and mandibular casts prior to testing. The recording materials—articulating paper and T-Scan III—were placed sequentially on the occlusal surface of the mandibular teeth of the model.

Methodology

Preliminary loading of casts was performed once to properly mate the casts and then again to ensure that the overshoot of load cell was an acceptable value. Then, the Bausch articulating paper (thickness, 0.04 mm), with red surface occluding the maxillary cast and blue surface occluding the mandibular cast, was held in place between the casts. The loading began before the dies were intercuspated until complete intercuspation at 25-N loads. Then, the readings on the displaying unit were recorded before returning to zero position to release the load. This procedure was repeated 2 more times, with each 3-tap trial comprising one test. Next, the paper markings left on the maxillary and mandibular casts were photographed with a 10-megapixel digital camera. The load was gradually increased from 25 N to 450 N, and the entire process was repeated.

Figure 1. Horseshoe-shaped, full arch, red-blue articulating paper (left) and articulating paper mark area (right).

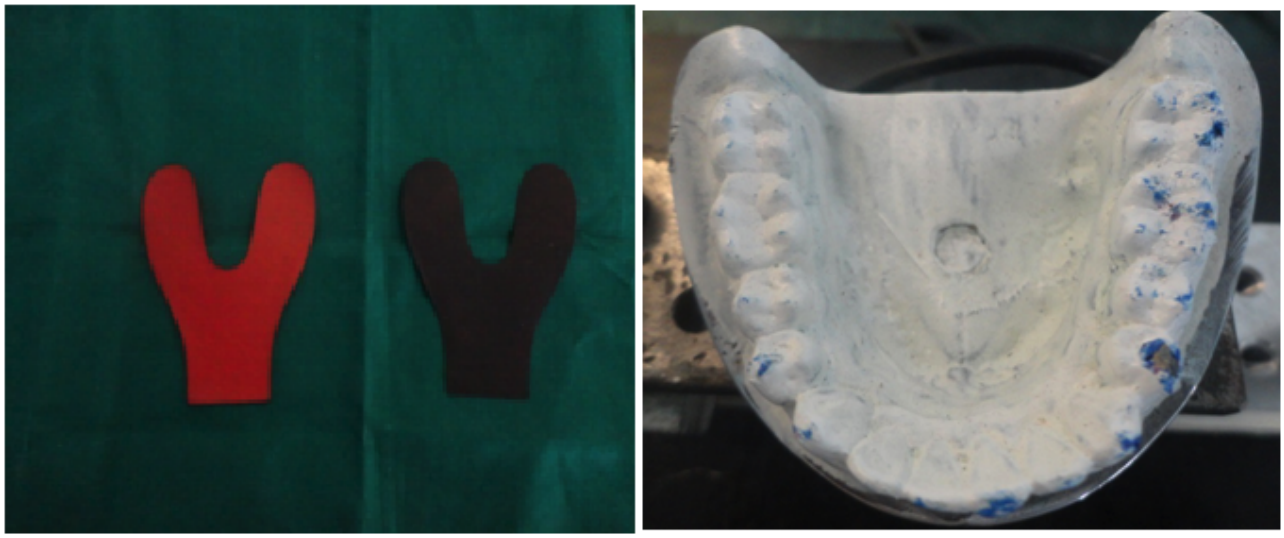

Figure 2. Metal maxillary and mandibular dies mounted on a jig.

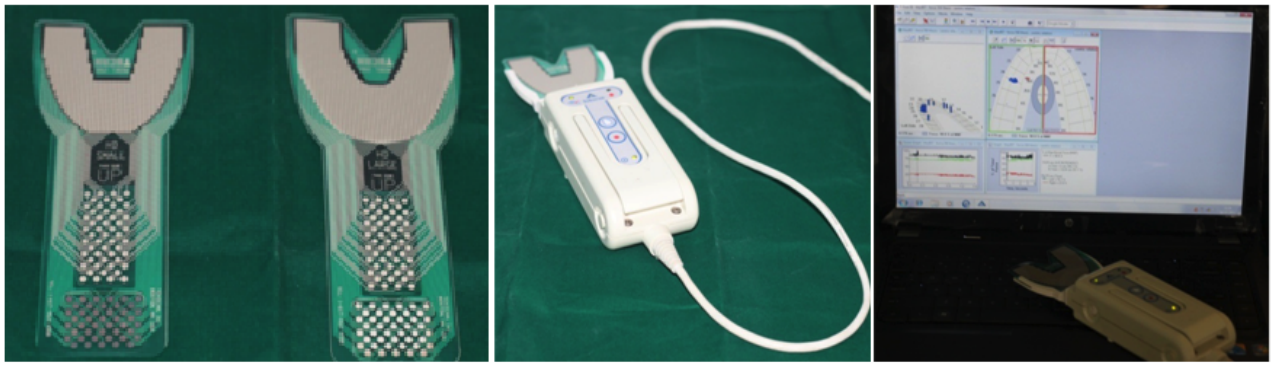

Recording Procedure Using T-Scan III

Prior to recording, the handle with a sensor (Figure 3) and arch support was placed between the maxillary and mandibular metal dies. The sensor was placed in such a way that it aligned centrally with the midline of the maxillary incisors. Then, the recording was initiated by depressing and releasing the recording button located on the top surface of the recording handle. After the handle button was pressed, the arch model was automatically created on the screen. When the sensor was placed between the two opposing dies at maximum intercuspation, the resultant reduction in electric resistance was translated into an image on the screen (Figure 4). We used MOTIC software (Motic microscopy, Hong Kong; accessed from the Department of Oral Pathology, The Oxford Dental College Bangalore), which has been designed to analyze and display tooth contact data as registered by the sensor (Figure 5). Next, the T-scan III was occluded between the metal dies and the force was loaded and recorded. The load was gradually increased from 25 N to 450 N, and the entire process was repeated. This procedure was repeated 2 more times, with each 3-tap trial comprising one test [11].

Image Analysis and Processing

Photographs of the paper markings left on the maxillary and mandibular casts resulting from each 3-tap trial were analyzed. We used a 10-mega pixel digital camera placed at a distance of 6 inches from the metal dies. The experimental design produced 100 photos for analysis. In all photographs, 6 prominent markings (indicating 6 contacts) were identified on the casts. Any other inconsistent occlusal markings were disregarded. The 6 distinct contact markings were analyzed using MOTIC software to magnify the markings. The markings were analyzed sequentially from contact numbers 1-6. A total of 180 (6 teeth × 10 force levels × 3 repetitions =180) marks were statistically analyzed. Furthermore, the photographs of T-Scan markings, which were displayed as an arch model on the screen, were analyzed using MOTIC software.

Calculation of the Size of the Largest Paper Mark per Photograph

We used a freehand sketcher (Adobe Photoshop CS4, San Jose, CA, USA) to magnify and calculate the paper mark surface area in photographic pixels of the largest and most prominent articulation paper mark found in a marked quadrant. MOTIC software was used to magnify the markings so that the freehand sketcher could be used to trace the boundary of the paper mark. The largest mark was outlined using MOTIC software outline sketcher command, which accessed the number of pixel count within the enclosed boundary (the freehand sketcher automatically calculates the number of pixels enclosed within the outlined area). Next, the tooth and the contact location of the largest paper mark in a quadrant were recorded in a spreadsheet for future data analysis.

Statistical Analysis

We performed descriptive statistical analysis in this study. Comparisons were performed using one-way analysis of variance (ANOVA), Student *t* test, and Pearson correlation coefficient method.

Figure 3. T-Scan sensor, USB handle with attached USB cable, and T-Scan system unit.

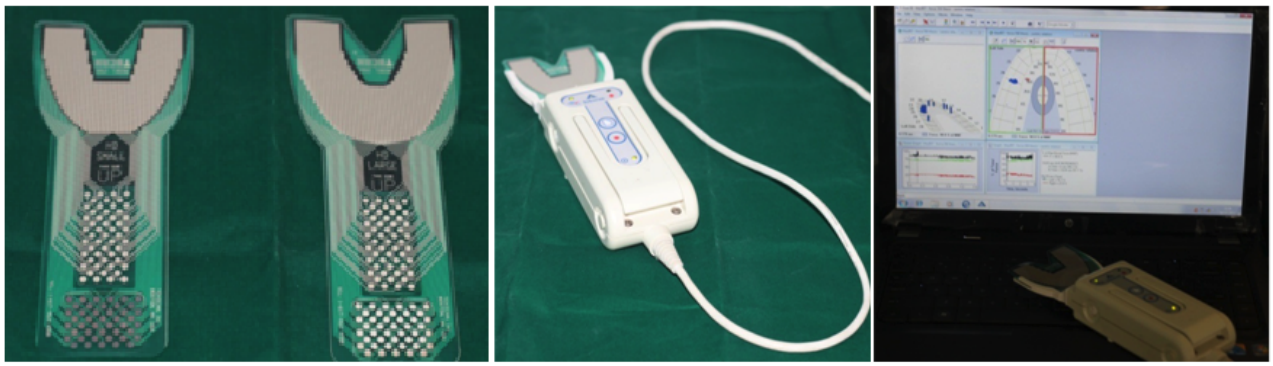

Figure 4. T-Scan contact markings.

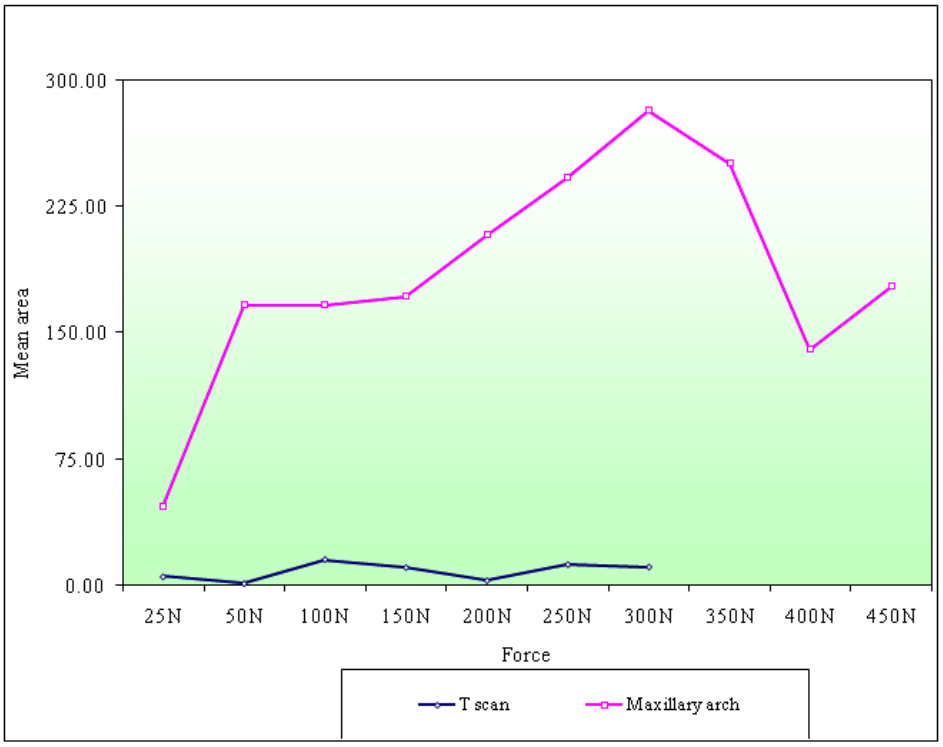

Figure 5. Image analysis using MOTIC software.

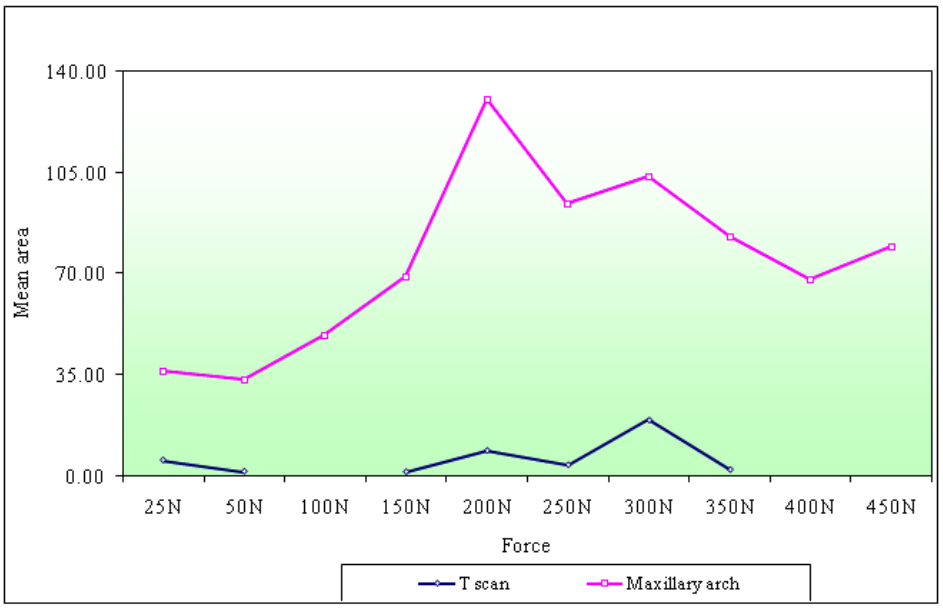

Results

Data were plotted for each of the 6 marks of the articulating paper and the marks that were evaluated using T-Scan. We plotted a best-fit curve and performed one-way ANOVA and Pearson correlation coefficient method. Data were grouped and plotted by each load level to calculate descriptive statistics. Because all teeth were subjected to the exactly same loads, Student *t* test was used to determine whether the mark areas were the same or significantly different at each load. During all tests, no gross observable paper failure was found; however, some local indentations or crinkling was observed as paper conformed to the shape of tooth edges. Furthermore, each T-Scan sensor was used for 10 test loads.

In the incisor region, the articulating paper mark area was maximum at a load of 300 N and was 282.50 μm^2, whereas with the T-Scan, the maximum area was 30.63 μm^2 at 100 N (Tables 1 and 2; Figure 6).

Table 1. Comparison of different forces with area (in micrometer square) marked with articulating paper in different teeth regions using one-way analysis of variance.

Force (N)	Left side canine, mean (SD)	Incisors, mean (SD)	Right side canine, mean (SD)	Premolar, mean (SD)	First molar, mean (SD)	Second molar, mean (SD)
25	58.00 (16.52)	46.67 (10.12)	36.00 (3.46)	75.67 (30.92)	50.17 (11.09)	37.33 (6.43)
50	55.67 (4.91)0	166.50 (48.48)	33.17 (7.94)	247.00 (26.51)	170.67 (48.91)	137.67 (27.32)
100	101.50 (8.67)	166.67 (36.94)	48.33 (21.94)	373.67 (86.77)	251.67 (55.99)	131.33 (29.26)
150	35.00 (7.94)	171.67 (32.52)	69.00 (3.46)	513.33 (69.95)	202.33 (59.47)	184.00 (11.27)
200	113.50 (16.86)	208.67 (7.51)	130.33 (30.14)	239.33 (44.46)	239.33 (44.46)	160.00 (21.28)
250	105.17 (8.95)	242.67 (29.87)	94.33 (20.31)	549.67 (32.75)	271.00 (20.22)	243.00 (29.55)
300	98.17 (15.25)	282.50 (78.38)	103.67 (10.50)	444.67 (34.20)	269.50 (62.93)	213.33 (25.11)
350	77.50 (10.76)	251.00 (89.00)	82.67 (1.53)	404.67 (60.05)	256.00 (42.79)	265.33 (15.70)
400	85.00 (11.95)	140.17 (28.65)	68.00 (8.72)	350.83 (35.76)	166.83 (41.12)	128.33 (22.81)
450	99.00 (7.76)	178.00 (36.37)	79.33 (6.03)	442.33 (37.87)	159.67 (28.22)	169.00 (43.14)
P value	<0.001	<0.001	<0.001	<0.001	<0.001	<0.001

Table 2. Comparison of different forces with area (in micrometer square) marked with T-Scan in different teeth regions using analysis of variance.

Force (N)	Left side					Right side			
	Second molar, mean (SD)	First molar, mean (SD)	Premolar, mean (SD)	Canine, mean (SD)	Incisors, mean (SD)	Incisors, mean (SD)	Canine, mean (SD)	Premolar, mean (SD)	First molar, mean (SD)
25	N/A[a]	N/A	N/A	10.90 (1.00)	10.40 (0.72)	N/A	N/A	N/A	N/A
50	N/A	N/A	15.37 (8.00)	3.03 (0.81)	2.47 (0.32)	N/A	N/A	N/A	N/A
100	N/A	21.00 (1.00)	N/A	N/A	30.63 (3.50)	N/A	N/A	N/A	N/A
150	N/A	13.47 (4.97)	3.60 (1.41)	2.67 (1.10)	21.33 (4.93)	N/A	N/A	N/A	N/A
200	N/A	20.33 (8.33)	21.67 (4.04)	15.33 (3.21)	N/A	6.00 (3.00)	2.23 (0.68)	2.70 (1.47)	N/A
250	N/A	30.20 (6.88)	19.67 (7.64)	7.50 (1.87)	N/A	24.67 (7.19)	N/A	N/A	N/A
300	N/A	15.53 (0.55)	21.97 (4.38)	38.70 (2.04)	21.90 (5.12)	N/A	N/A	2.87 (1.36)	N/A
350	8.30 (8.44)	20.63 (5.12)	16.10 (2.95)	N/A	N/A	N/A	4.20 (0.95)	N/A	N/A
400	17.73 (1.00)	41.33 (4.51)	37.67 (7.77)	37.67 (11.68)	21.67 (5.03)	N/A	24.67 (6.81)	13.10 (1.65)	28.60 (2.62)
450	19.30 (5.52)	49.97 (6.41)	56.37 (7.42)	52.87 (12.27)	27.73 (3.66)	N/A	11.10 (3.92)	30.53 (2.38)	31.83 (1.60)

[a]N/A: not applicable.

Figure 6. Comparison between results with articulating paper and T-Scan for applied load in the incisor region.

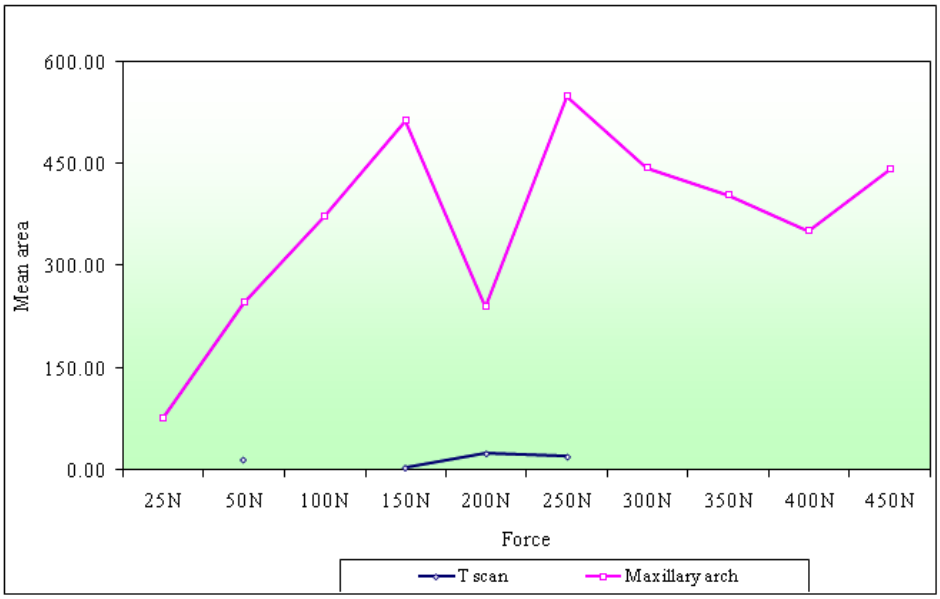

Figure 7. Comparison between results with articulating paper and T-Scan for applied load in the canine region.

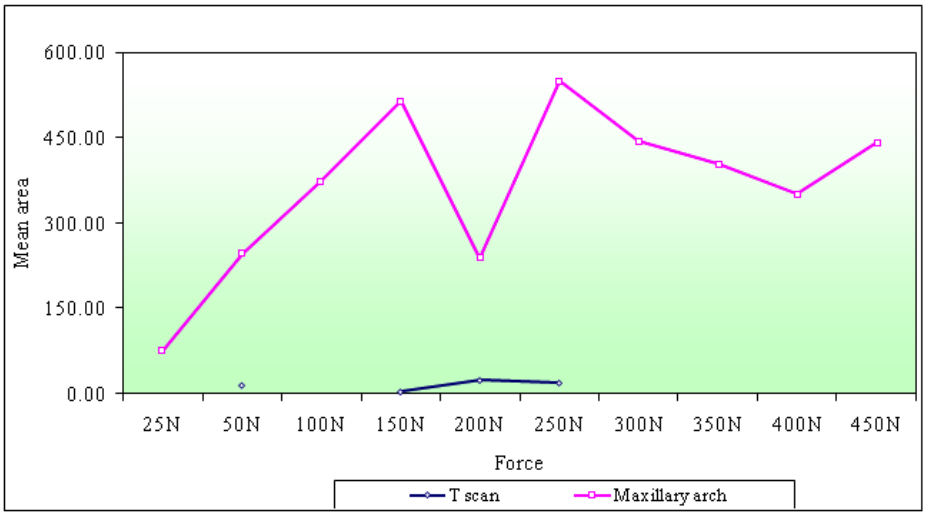

The size of the mark area was approximately 9 times greater with the articulating paper than with the T-Scan. In the canine region (Tables 1 and 2; Figure 7), the articulating paper mark area was maximum at 200 N and was 130.33 μm^2, whereas with the T-Scan, the maximum area was 52.87 μm^2 at 450 N. The mark area with the articulating paper was approximately 2 times greater than that with the T-Scan. In the premolar region (Tables 1 and 2; Figure 8), the articulating paper mark area was maximum at 250N and was 549.67 μm^2, whereas with the T-Scan, the maximum area was 56.37 μm^2 at 450 N. The mark area with the articulating paper was approximately 9 times greater than that with the T-Scan. In the first molar region (Tables 1 and 2; Figure 9), the articulating paper mark area was maximum at 250 N and was 271 μm^2, whereas with the T-Scan, the maximum area was 49.97 μm^2 at 450 N. The mark area with the articulating paper was approximately 5 times greater than that with the T-Scan. In the second molar region (Tables 1 and 2; Figure 10), the articulating paper mark area was maximum at 350 N and was 265.33 μm^2, whereas with T-Scan, the maximum area was 19.30 μm^2 at 450 N. The mark area with the articulating paper was approximately 10 times greater than that with the T-Scan.

Figure 8. Comparison between results with articulating paper and T-Scan for applied load in the first premolar region.

Figure 9. Comparison between results with articulating paper and T-Scan for applied load in the first molar region.

Figure 10. Comparison between results with articulating paper and T-Scan for applied load in the second molar region.

Figure 11. Comparison between results with articulating paper and T-Scan for applied load in the first molar region.

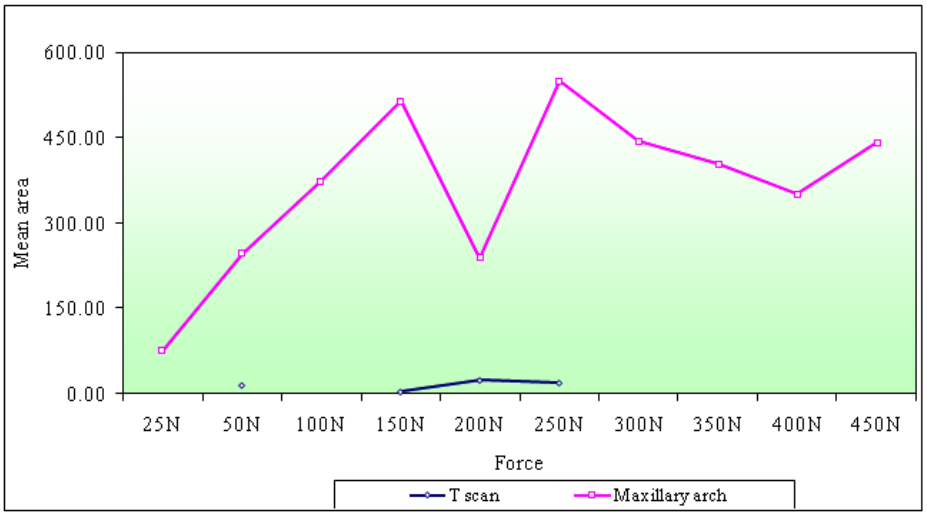

Figure 12. Comparison between results with articulating paper and T-Scan for applied load in the second molar region.

Discussion

Principal Findings

Articulating papers are the most frequently used qualitative indicators to locate the occlusal contacts intraorally; their basic constituents are a coloring agent and a bonding agent between the two layers of the film [10]. On occlusal contact, the coloring agent is expelled from the film, and the bonding agent binds it on to the tooth surface [12]. On heavy contacts (ie, greatest masticatory pressure), more color is squeezed out, resulting in dark marks. When light contacts are made (ie, slight masticatory pressure), less color is expelled, resulting in light marks. On heavy contacts (ie, greatest masticatory pressure), more color is squeezed out, resulting in dark marks. When light contacts are made (ie, slight masticatory pressure), less color is expelled, resulting in light marks. The selected marks to adjust are generally chosen on the basis of their appearance characteristics. The characteristic marking is observed as a central area that is devoid of the colorant and surrounded by a peripheral rim of the dye; this region is called “target” or “iris” owing to its appearance, and it denotes the exact contact point. The density of these markings does not denote the force of the contact; instead, heavier contacts tend to spread the mark peripheral to the actual location of the occlusal contact. Only the central portion in heavy contact areas indicates the interference that requires correction [12]. We evaluated this hypothesis to determine whether a relationship exists between the applied occlusal load and the size of the markings produced from tooth contact when a clinically used dental articulating paper and T-Scan are interposed alternatively.

The results of this study suggest that there is no correlation between the mark area and the applied occlusal load. With the articulating paper, we observed false-positive results, which is in accordance with the results of a study conducted by Kerstein and Qadeer [13,14] who attempted to correlate the occlusal force to the paper mark size. Hence, we can conclude that the characteristics of the paper mark appearance do not describe the amount of occlusal load present on a given tooth. In addition, this study proved that the incremental load increase did not result in an equal increase in mark area size on any individual

contact; furthermore, the maximum area recorded was at the maximum force with T-Scan, which is in accordance with Carey et al [10], Kim [9], Reza and Neff [15], and Garrido et al [16]. This computerized occlusal analysis showed that similar-sized and widely distributed marks did not indicate a measurably simultaneous occlusal scheme; furthermore, despite their similar sizes, those same marks exhibited a wide range of forces.

Afrashtehfar and Qadeer [17] have reported that the computerized occlusal analysis system provides quantifiable force and time variance in a real-time window from the initial tooth contact to the maximum intercuspation, therefore, providing valuable information. Bozhkova [18] reported that the T-Scan system provides a very accurate way of determining and evaluating the time sequence and force magnitude of occlusal contacts by converting qualitative data into quantitative parameters and displaying them digitally. The system is a useful clinical method that eliminates a biased, subjective evaluation of the occlusal and articulating relations on the part of an operator, which is in accordance with the results of our study [18].

An assumption made regarding the articulating paper labeling is that the size and color intensity describe forceful contact. A broad, dark-colored contact is perceived as a forceful contact. A possible explanation for this relationship between the size of the contact and its force content is that the applied pressure of the occlusal force is measured relative to its surface area as follows: pressure applied force/surface area

Broad contacts dissipate force over a large area, resulting in low-pressure concentration, whereas a small contact will dissipate the occlusal force over a small area. Thus, the smaller the surface area that receives a given force, the more the pressure. A computerized analysis may reveal that dentists have been misreading the size of the articulating paper labeling by reading it inversely. Therefore, large or broad contacts are representative of low pressure, while small contacts represent high pressure. The only data that appear to be obtainable with articulating paper labeling are occlusal contact location and surface area. In addition, color intensity, size of labeling, and microscratch labeling reveal the presence of an occlusal contact without revealing any description of the force content or time sequence data.

Limitations

Only one type of commonly used articulating paper was used in this study; thus, extrapolations of the behavior of other paper or ribbon types cannot be universally made. The results do not necessarily reflect other types and thicknesses of different commercially available articulating papers. Articulating paper is very delicate and tends to smudge even with finger pressure, giving false-positive markings. In this study, the complexities of the anatomical and physiological aspects of the human teeth, which rest in the hydrodynamic environment of the periodontal ligament, were purposefully not duplicated. The final limitation was subjectively defining and sketching the boundary of the mark area using MOTIC software; it was easier to identify the boundaries of the blue markings than those of the red markings.

Conclusion

In this bench analysis, we could not find a linear relationship between the applied load and the articulating paper mark area because of the high degree of mark area variability observed at each test load across differing teeth and contacts. These findings question the long-standing dental premises that the size of an articulating paper mark indicates its load content. Contact marking using T-Scan for an applied occlusal load helped conclude that the mark area increased with an increase in the load.

From the results of this study, we can conclude that the combination of these two different mediums can guide the occlusal adjustment procedure to result in a measurable bilateral simultaneous occlusal contact sequence. Furthermore, the size of an articulating paper mark may not be a reliable predictor of the actual load content within the occlusal contact, and T-Scan gives more predictable results of the actual load content within the occlusal contact. Hence, it is imperative that dentists realize that the articulating paper mark size is subject to interpretation and could be an unreliable method to use for occlusal equilibration

Conflicts of Interest

None declared.

References

1. Forrester SE, Presswood RG, Toy AC, Pain MTG. Occlusal measurement method can affect SEMG activity during occlusion. J Oral Rehabil 2011 Sep;38(9):655-660. [doi: 10.1111/j.1365-2842.2011.02205.x] [Medline: 21314708]
2. Saraçoğlu A, Ozpinar B. In vivo and in vitro evaluation of occlusal indicator sensitivity. J Prosthet Dent 2002 Nov;88(5):522-526. [doi: 10.1067/mpr.2002.129064] [Medline: 12474003]
3. Manes WL, Podoloff R. Distribution of occlusal contacts in maximum intercuspation. J Prosthet Dent 1989 Aug;62(2):238-242. [Medline: 2760866]
4. Glickman I. Clinical Periodontics. 5th ed. Philadelphia: Saunders and Co; 1979:951.
5. McNeill C, editor. Science practice of occlusion. Carol Stream: Quintessence Publishing; 1997:421-421.
6. Okeson J. Management of temporomandibular disorders and occlusion, 5th ed. St Louis: Mosby and Co; 2003:416, 418, 605.
7. Kleinberg I. Occlusion practice and assessment. Oxford: Knight Publishing; 1991:128.

8. Smukler H. Equilibration in the natural and restored dentition: a rational basis for and technique of occlusal equilibration. Chicago: Quintessence Publishing; 1991:110.
9. Kim JH. Computerized Occlusion Using T-Scan III. 2016. Computerized Occlusal Analysis Utilizing the T-Scan III System URL: http://www.tscan.nl/wp-content/uploads/2016/12/DTL-T-Scan-Clinical-eBook.pdf [WebCite Cache ID 72FAeHmqJ]
10. Carey JP, Craig M, Kerstein RB, Radke J. Determining a relationship between applied occlusal load and articulating paper mark area. Open Dent J 2007;1:1-7 [FREE Full text] [doi: 10.2174/1874210600701010001] [Medline: 19088874]
11. Tekscan: T-Scan III User Manual. South Boston URL: http://www.dlmedica.it/contenuti/prodotti/download/91/T-SCAN%20III%20Applicazioni%20cliniche%2FTscan_Manual.pdf [accessed 2018-09-06] [WebCite Cache ID 72FBDjxMm]
12. Babu RR, Nayar SV. Occlusion indicators: A review. J Indian Prosthodont Soc 2007;7(4):170. [doi: 10.4103/0972-4052.41066]
13. Bausch Articulating and Occlusion Test Materials Manual. 2017. URL: http://www.bausch.fm/bauschweb/dwnld/BauschEN.pdf [WebCite Cache ID 72FB0BDHI]
14. Qadeer S, Kerstein R, Kim RJY, Huh JB, Shin SW. Relationship between articulation paper mark size and percentage of force measured with computerized occlusal analysis. J Adv Prosthodont 2012 Feb;4(1):7-12 [FREE Full text] [doi: 10.4047/jap.2012.4.1.7] [Medline: 22439094]
15. Reza MM, Neff PA. Reproducibility of occlusal contacts utilizing a computerized instrument. Quintessence Int 1991 May;22(5):357-360. [Medline: 1924688]
16. Garrido García VC, García CA, González SO. Evaluation of occlusal contacts in maximum intercuspation using the T-Scan system. J Oral Rehabil 1997 Dec;24(12):899-903. [Medline: 9467991]
17. Afrashtehfar KI, Qadeer S. Computerized occlusal analysis as an alternative occlusal indicator. The Journal of Craniomandibular & Sleep Practice 2016;34(1):52-57 [FREE Full text] [doi: 10.1179/2151090314Y.0000000024]
18. Bozhkova TP. The T-SCAN System in Evaluating Occlusal Contacts. Folia Medica 2016;58(2):122-130. [doi: 10.1515/folmed-2016-0015]

Abbreviations

ANOVA: analysis of variance

Edited by G Eysenbach; submitted 24.06.18; peer-reviewed by S Jagadeesh, G Madhav; comments to author 01.08.18; revised version received 12.08.18; accepted 13.08.18; published 02.10.18.

Please cite as:
Reddy S, Kumar PS, Grandhi VV
Relationship Between the Applied Occlusal Load and the Size of Markings Produced Due to Occlusal Contact Using Dental Articulating Paper and T-Scan: Comparative Study
JMIR Biomed Eng 2018;3(1):e11347
URL: http://biomedeng.jmir.org/2018/1/e11347/
doi:10.2196/11347
PMID:

Publisher:
JMIR Publications
130 Queens Quay East.
Toronto, ON, M5A 3Y5
Phone: (+1) 416-583-2040
Email: support@jmir.org